PALEOMAGNETISM OF THE CRETACEOUS GALULA FORMATION AND IMPLICATIONS FOR VERTEBRATE EVOLUTION

Sarah J. Widlansky ^{a*}, William C. Clyde ^a, Patrick M. O'Connor ^{b,c}, Eric M. Roberts ^d,

Nancy J. Stevens ^{b,c}

^aDepartment of Earth Sciences, University of New Hampshire. Durham, New Hampshire, 03824, USA, sjw2008@wildcats.unh.edu; will.clyde@unh.edu

^bDepartment of Biomedical Sciences, Ohio University Heritage College of Osteopathic Medicine, 228 Irvine Hall, Athens, Ohio, 45701, U.S.A., oconnorp@ohio.edu; stevensn@ohio.edu

^cOhio Center for Ecology and Evolutionary Studies, Irvine Hall, Ohio University, Athens, OH, 45701, U.S.A.

^dDepartment of Geosciences, James Cook University, Townsville, Queensland, Australia., eric.roberts@jcu.edu.au

* Corresponding author. Tel.: +1 561-670-4782

E-mail address: sjw2008@wildcats.unh.edu

Abstract

This study uses magnetostratigraphy to help constrain the age of the paleontologically important Galula Formation (Rukwa Rift Basin, southwestern Tanzania). The formation preserves a Cretaceous vertebrate fauna, including saurischian dinosaurs, a putative gondwanatherian mammal, and notosuchian crocodyliforms, but its precise age within the Cetaceous is unknown. With better dating, the Galula Formation and its fossils help fill a temporal gap in our understanding of vertebrate evolution in continental Africa, enabling better evaluation of competing paleobiogeographic hypotheses concerning faunal exchange throughout Gondwana during the Cretaceous. Paleomagnetic samples for this study were collected from the Namba (higher in section) and Mtuka (lower in section) members of the Galula Formation and underwent stepwise thermal demagnetization. All samples displayed a strong normal magnetic polarity overprint, and maximum unblocking temperatures at approximately 690 °C. Three short reversed intervals were identified in the Namba Member, whereas the Mtuka Member lacked any clear reversals. Given the relatively limited existing age constraints, one interpretation correlates the Namba Member to Chron C32. An alternative correlation assigns reversals in the Namba Member to recently proposed short reversals near the end of the Cretaceous Normal Superchron (Chron C34), a time that is traditionally interpreted as having stable normal polarity. The lack of reversals in the Mtuka Member supports deposition within Chron C34. These data suggest that the Namba Member is no older than Late Cretaceous (Cenomanian-Campanian), with the Mtuka Member less well constrained to the middle Cretaceous (Aptian-Cenomanian). The paleomagnetic results are supported by the application of fold and reversal tests for paleomagnetic stability, and paleomagnetic poles for the

Namba (246.4°/77.9°, α₉₅ 5.9°) and Mtuka (217.1°/72.2°, α₉₅ 11.1°) members closely matching the apparent polar wander path for Africa during the Late Cretaceous. These results confidently indicate a Late Creteceous age assignment for the Namba Member of the Galula Formation, a unit that has yielded key crocodyliform (e.g., *Pakasuchus*; *Rukwasuchus*) and dinosaur (e.g., *Rukwatitan; Shingopana*) fossils from eastern Africa.

Keywords: Paleomagnetism, Late Cretaceous, Africa, Tanzania, Rukwa Rift Basin

1. Introduction

The geological and biological history of Africa is poorly known when compared to that of other continents, and this is especially true during the Cretaceous – Paleogene interval. Understanding faunal evolution in Africa during this time is critical for testing a variety of hypotheses that identify Africa as an important link among Gondwanan landmasses and essential for understanding the pattern of Gondwanan continental breakup during the Cretaceous (e.g., Sampson et al., 1998; Sereno et al., 2004; Krause et al., 2006). For example, a Gondwanan origin has been hypothesized for several animal groups, including placental mammals (e.g., Stanhope et al., 1998; Eizirik et al., 2001; Murphy et al., 2001) but the fossil record is currently insufficient for testing this idea. Indeed, the striking lack of fossil material from Africa prior to the Neogene has been referred to as the "African Gap" (O'Connor et al., 2006) and it remains unclear whether this reflects sampling bias or a relative lack of deposition during this period. Ongoing geological and paleontological field research in the Rukwa Rift Basin of southwestern Tanzania has identified a rich assemblage of sedimentary deposits, in addition to vertebrate and invertebrate fossils, that span this poorly understood interval and provide a means to directly test several hypotheses concerning the role of Africa in global paleobiogeography during this time (Krause et al., 2003; O'Connor et al., 2006, 2010; Stevens et al., 2006, 2008, 2009a, 2009b, 2013; Feldmann et al., 2007; Gottfried et al., 2009; Roberts et al., 2010; Gorscak et al., 2014, 2017).

The Rukwa Rift Basin is an extensional sedimentary basin, roughly 300 km long and 50 km wide and located at approximately 8°S, 32°E (Chorowicz, 2005; Roberts et

al., 2010). The basin follows a general northwest – southeast trend and occupies a local zone of weakness associated with the Proterozoic Ubendian mobile belt, bordering the stable Tanzania Craton to the northeast (Figure 1). The Rukwa Rift Basin is one of several sedimentary basins making up the Western Branch of the modern East African Rift System (EARS) and preserves thick sequences of continental sedimentary rocks and associated fossil assemblages.

Early geological exploration of the rift basin was primarily focused on hydrocarbon and resource exploration (e.g., Grantham et al., 1958; McKinlay, 1965; Peirce and Lipkov, 1988). Although initial hydrocarbon recovery was unsuccessful, it led to the recognition of three major sequences of sediment deposition in the Rukwa Rift Basin: the upper Carbonifierous – Permian Karoo Supergroup, the Cretaceous – Paleogene Red Sandstone Group, and the Neogene Lake Beds Formation (Wescott et al., 1991; Kilembe and Rosendahl, 1992; Roberts et al., 2004).

Establishment of the Rukwa Rift Basin Project in 2002 has largely focused efforts on understanding the Red Sandstone Group (RSG), as this sequence preserves important fossil vertebrate faunas (e.g., O'Connor et al., 2006, 2010; Stevens et al., 2008, 2013). Roberts et al. (2010) proposed a division of the RSG into two formations: the Cretaceous Galula Formation and the Oligocene Nsungwe Formation, based on the presence of temporally disparate faunas and differences in lithology, in addition to longstanding discrepancies concerning the age of the Red Sandstone Group (see Roberts et al., 2010 for discussion). Each of these time intervals is very poorly represented in the geologic record of sub-Saharan Africa, so the numerous RSG

exposures in the Rukwa Rift Basin offer an important opportunity for advancing understanding of the geological and evolutionary history of continental Africa.

Obtaining a precise age for the fossil-bearing Galula Formation has been hindered by the shortage of primary volcanic material for radiometric dating. The age of the Galula Formation is important for reconstructing the timing of faunal and landscape changes in eastern Africa, particularly in clarifying paleobiogeographic patterns associated with the breakup of Gondwana during the Cretaceous (e.g., Sereno et al., 2004; Krause et al., 2006; Gorscak et al., 2014, 2017; Sertich and O'Connor, 2014; Gorscak and O'Connor, 2016). As such, a well-constrained age for the Galula Formation is significant in addressing paleobiological questions at regional and global scales.

This study applies magnetic reversal stratigraphy to sedimentary rocks from the Galula Formation to construct a more robust temporal framework for the unit, facilitating comparisons with potentially correlative sequences in eastern Africa and beyond. In constraining the age of the Galula Formation independently from vertebrate biostratigraphy, this study provides the first direct age determination for the Namba and Mtuka members.

2. BACKGROUND AND PREVIOUS WORK

2.1 Galula Formation

2.1.1 Stratigraphy and Sedimentology

Roberts et al. (2010) provided a detailed sedimentological description of the Galula Formation and described it as a "sequence of red, pink, purple and occasionally white colored sandstones, conglomerates and mudstones" (Roberts et al., 2010, p. 187). The Galula Formation includes two members: the lower Mtuka Member, and the upper Namba Member (Roberts et al., 2010). The Mtuka Member of the Galula Formation generally displays more heterolithic lithologies with abundant coarse sandstones and conglomerates interbedded with paleosol mudstones. The Namba Member lithology is more homogenous than the Mtuka Member, dominated by abundant fine-to-medium grained sandstones with fewer overbank mudstone deposits (Roberts et al., 2010).

The Galula Formation, as a whole, is interpreted to represent a Cretaceous braided fluvial system. U-Pb detrital zircon provenance and paleocurrent analyses suggest a general northwest flow direction during the Cretaceous, with sediment sourced from topographically high regions of Zambia, Malawi and Mozambique and drainage ultimately reaching the Congo Basin (Roberts et al., 2012). A shift in sediment provenance between the Mtuka and Namba members from proximal to more distal sources is interpreted to reflect a slowing rate of basin subsidence and rift flank uplift during the Cretaceous (Roberts et al., 2012). Several lines of sedimentological evidence suggest the Mtuka – Namba Member transition may record a subtle shift in paleoclimate from a seasonally dry, sub-arid climate in the Mtuka Member to a wetter sub-humid climate in the Namba Member (Roberts et al., 2010). Support for this interpretation comes from a noticeable shift from an illite and smectite-dominated clay mineral

assemblage in the Mtuka Member, to a kaolinite-dominated assemblage in the Namba Member, in addition to the prevalence of pedogenic carbonate in the Mtuka Member that is absent in the Namba Member (Choh, 2007; Roberts et al., 2010).

2.1.2 Age Estimates for the Galula Formation

Dateable volcanic deposits from the Galula Formation have not been recovered despite evidence supporting deposition concurrent with active tectonism (Roberts et al., 2010). A Cretaceous age for the unit has been assigned based on the fossil assemblage (O'Connor et al., 2006), sedimentological and general faunal similarities with the ~Aptian Dinosaur Beds of Malawi, and evidence for Galula deposition coeval with emplacement of local carbonatite intrusive bodies between ~116 – 96 Ma (Fawley and James, 1955; Roberts et al., 2010).

Although much of the early uncertainty concerning the age of the RSG has been resolved by recognizing two distinct formations (Roberts et al., 2010), uncertainty remains concerning the precise age of the Galula Formation within the Cretaceous. Detrital zircon analyses reveal a population of approximately 150 Ma grains, suggesting a maximum depositional age in the Late Jurassic (Roberts et al., 2012). Recently, a single ~118 Ma grain was recovered from the upper Namba Member (E. M. Roberts, unpublished data), suggesting deposition after the middle Early Cretaceous if supported by subsequent observations. Palynological evidence from sediment cores have yielded mixed findings. Recovery of pollens with a Middle Jurassic-to-middle Cretaceous range (Classopollis classoides and Callialasporites dampieri; Kilembe and Rosendahl, 1992)

could constrain Galula Formation deposition to the Early – middle Cretaceous, although it has been proposed that these pollens may reflect contamination from Cretaceous bentonite used in drilling wells where samples were recovered (Mliga, 1994; Morley et al., 1999).

Data from initial exploratory wells suggest sediment deposition occurred in the basin between 180 – 100 Ma (Mliga, 1994) using the Faust (1951) method, with age estimates based on the relationship of seismic velocity and burial depth. Evidence for soft sediment deformation in the upper portion of the Namba Member suggests deposition occurred during a period of active tectonism (Hilbert-Wolf et al., 2016), and is generally consistent with deposition occurring simultaneously with local emplacement of Cretaceous carbonatite. This is further supported by the observation of cross-cutting relationships between the Galula Formation and the Panda Hill Carbonatite Complex, including a carbonatite dike intruding into, and appearing to be truncated by, Galula Formation sandstones (Fawley and James, 1955; Roberts et al., 2010). K-Ar dating of phlogopite in the Panda Hill carbonatite gives an age of 113 ± 6 Ma (Snelling, 1965), potentially constraining Galula deposition to the Late Cretaceous, although more recently applied ⁴⁰Ar/³⁹Ar geochronology suggests a Jurassic (165.7 ± 1.3 Ma) age for Panda Hill (Mesko et al., 2014). It should also be noted that Roberts et al. (2012), Stevens et al. (2013) and most recently, Spandler et al. (2016), each reported new ages and expanded evidence for carbonatite tuffs in the overlying Oligocene Nsungwe Formation of the RSG. The source of these carbonatite volcanics has yet to be identified, but reactivation of the Panda Hill carbonatite is one of the more likely sources. Together with the recent work by Mesko et al. (2014) showing that at least

portions of both the Panda Hill and Mbalizi carbonatites were erupted during the Jurassic, this suggests that the age and nature of cross-cutting relationships between carbonatite volcanics and the Galula Formation must be considered with great caution at this stage and highlights a need for more comprehensive dating of that unit. Apatite-fission track dating from the Rukwa Rift flanks indicate that a period of active rifting occurred in the Late Jurassic – Early Cretaceous (Van der Beek et al., 1998), and is generally consistent with observations elsewhere in Africa for the Early – middle Cretaceous (Roberts et al., 2010).

2.1.3 Vertebrate Fauna and Implications for Cretaceous Paleobiogeography

Vertebrate fossils from the Galula Formation are generally found as isolated elements, although some associated and semi-articulated to articulated skeletons have been discovered (O'Connor et al., 2006, 2010). Representatives of several key vertebrate groups have been described from the Galula Formation (Table 1), including sauropod and non-avian theropod dinosaurs (O'Connor et al., 2006; Gorscak et al., 2014, 2017), notosuchian and peirosaurid crocodyliforms (O'Connor et al., 2010; Sertich and O'Connor, 2014), ceratodontid and osteoglossomorph fishes (Gottfried et al., 2009; O'Connor et al., 2006) and turtle elements of unknown taxonomic affinity.

Fossils from the Namba Member exhibit affinities with other eastern African Cretaceous localities (e.g., the Malawi Dinosaur Beds), and taxa such as titanosaurian sauropod dinosaurs and notosuchian crocodyliforms have been used as general biostratigraphic support for a middle Cretaceous (120 – 90 Ma) age interpretation for the

unit (O'Connor et al., 2006; Roberts et al., 2010). Le Loeuff et al. (2012), however, suggest a later Cretaceous age for the formation based on the presence of derived titanosaurs (Gorscak et al., 2017), megaloolithid eggshells (Gottfried et al., 2004) and a mammal provisionally assigned to Gondwanatheria (Krause et al., 2003).

The Cretaceous reflects an important interval in the breakup of Gondwana with profound effects on later faunal distribution patterns. Paleomagnetic interpretations of the precise timing of plate movements during the middle Cretaceous are hindered by the long stable signal of the Cretaceous Normal Superchron (CNS), a ~38 Myr period of normal magnetic polarity from approximately 121 – 83 Ma. The lack of seafloor magnetic anomalies spanning this time makes it difficult to constrain the onset, rate, and progression of rifting between continents during the CNS. Consequently, the precise timing of separation between Africa and other Gondwanan landmasses is poorly resolved. To complicate matters, the fossil record from this interval on continental Africa is sparse, with the majority of Cretaceous exposures documented in northwestern Africa (Fig. 1). Cretaceous fossil localities are less common from Africa south of the equator, notably including the ~Aptian Dinosaur Beds of Malawi (e.g., Jacobs et al., 1990), the Berriasian-Valanginian Kirkwood Fauna of South Africa (e.g., De Klerk et al., 2000), the temporally well-constrained Turonian Tadi site of Angola (Mateus et al., 2011), and the Galula Formation of southwestern Tanzania that is the focus of this study.

A traditional view of the breakup of Gondwana has rifting beginning with the separation of "East Gondwana" (Indian subcontinent, Madagascar, Australia and Antarctica) from "West Gondwana" (South America and Africa) as the Indo-Madagascar block began to separate from Africa in the Late Triassic to Early Jurassic, with support

for seafloor spreading between Africa and Madagascar initiating by the late Middle Jurassic and a narrow seaway separating the two by approximately 160 Ma (Coffin and Rabinowitz, 1988; Lawver et al., 1992). Rifting between South America and Africa in "West Gondwana" began in the Early Cretaceous with spreading in the South Atlantic progressing northward. Evidence from seafloor magnetic anomalies and marine fossils suggest there was a complete seaway separating South America and Africa by ~100 Ma (Channell et al., 1995; Maisey, 2000; Néraudeau and Mathey, 2000; Granot and Dyment, 2015). Similarly, δ^{18} O from benthic foraminifera indicates a general cooling associated with the formation of intermediate and deep-water masses between South America and Africa by ~95 Ma (Friedrich et al., 2012; Granot and Dyment, 2015).

Of particular interest is documenting the biogeographic isolation of each Gondwanan landmass, when faunal exchange with other landmasses ceased. Historically, two primary hypotheses have emerged to explain patterns in biotic and geophysical data from Gondwana. These have become known as the "Africa first" and "pan-Gondwana" hypotheses, and reflect differing ideas concerning faunal exchange within Gondwana through the end of the Mesozoic.

The "Africa first" hypothesis, initially developed by Krause et al. (1997, 1999, 2006) and expanded during later studies (e.g., Sampson et al., 1998; O'Connor et al., 2006), argues that Africa was the first Gondwanan continent to become isolated by circum-continental seaways, becoming completely separated from the rest of Gondwana by the end of the Early Cretaceous (~100 Ma). This view posits that faunal exchange between the Indian subcontinent, Madagascar, Antarctica and South America persisted into the Late Cretaceous. This idea finds support in the strong similarities

among fossil taxa (including crocodyliforms, non-avian dinosaurs, and mammals) on Gondwanan continents exclusive of Africa during the Campanian – Maastrichtian (Krause et al., 2006). Geophysical models suggest that the Kerguelen Plateau and Gunnerus Ridge may have acted as land bridges facilitating exchange between the "East Gondwana" continents, with South American faunal exchange maintained through its connection with Antarctica into the Paleogene (Lawver et al., 1992; Hay et al., 1999).

The "pan-Gondwana" hypothesis (Sereno et al., 2004) argues that all Gondwanan landmasses maintained faunal exchange through the Early Cretaceous, until approximately 100 – 90 Ma. At this time, connections between Indo-Madagascar and Antarctica, Antarctica and South America, and South America and Africa were terminated nearly simultaneously, in a scenario more consistent with the paleogeographic reconstructions of Scotese (2001). Support for this hypothesis comes from the first discovery of abelisauroid theropods in Africa, a group well-documented in Upper Cretaceous deposits of South America (e.g., Bonaparte and Novas, 1985), India (e.g., Wilson et al., 2003) and Madagascar (e.g., Sampson et al., 1998) and suggests that faunal exchange was maintained between these landmasses closer to 95 Ma.

These historical hypotheses (summarized in detail by Krause et al., 2006) offer testable predictions as a more robust African fossil record emerges. The "Africa first" hypothesis predicts general similarity between African taxa and those from other Gondwanan continents until ~100 Ma. At this time, the African fauna would progressively become more endemic, with the remaining landmasses retaining faunal continuity until approximately 80 Ma. In contrast, the "pan-Gondwana" hypothesis

predicts a cosmopolitan faunal distribution across Gondwana until after 90 Ma, followed by a significant divergence in vertebrate faunas on each landmass.

Recent interpretations of the fossil record, combined with refined perspectives offered from geophysical data and paleogeographical modelling (Ali and Krause, 2011) suggest that the Kerguelen Plateau and Gunnerus Ridge are unlikely to have provided sufficient subaerial exposure to allow for dispersal of obligate terrestrial taxa among continents during the Late Cretaceous. Rather, the similar vertebrate faunas of Madagascar, South America and India during the Campanian – Maastrichtian are interpreted to reflect cosmopolitanism of the groups across Gondwana in general the Early Cretaceous, with long ghost lineages and a significant sampling bias (with minimal data from the African continent) fueling patterns observed in the Late Cretaceous. This idea is supported by stratigraphically calibrated phylogenies of major terrestrial vertebrate clades from the Cretaceous of Gondwana, including abelisauroid theropods, titanosaurian sauropods and notosuchian crocodyliforms, where the minimum divergence times estimated for each of the clades pre-dates the end of the Early Cretaceous and isolation of these continents (Ali and Krause, 2011). Contemporary research continues to evolve as considerations regarding the distribution of continental vertebrates from Africa, and Eurogondwana more generally, grow with increased sampling from selected areas (e.g., Morocco, Egypt; Longrich et al., 2017; Sallam et al., In Press) and evolving interpretations of the African continental vertebrate fossil record (e.g., Ezcurra and Agnolin, 2012).

2.2 Previous Paleomagnetic Studies from the Cretaceous of Africa

To date, no comprehensive paleomagnetic studies have been conducted for the Galula Formation in the Rukwa Rift Basin. Nairn (1964) conducted a preliminary paleomagnetic study on what were then identified as "Cretaceous red sandstones" from the Songwe River valley, though early confusion of Mesozoic and Cenozoic lenses in that region obscure the relevance of that work for elucidating the age of the Galula Formation. Moreover, no attempt was made to isolate a primary characteristic remanent magnetization (ChRM) from these samples, yielding ambiguous interpretations. Nyblade et al. (1993) conducted a paleomagnetic study of Permian Karoo rocks from Tanzania and reported an anomalous paleomagnetic pole position more consistent with a Late Cretaceous age from siltstone in the Songwe – Kiwira region (correlated to bed K5, following the stratigraphy of Stockley (1932)). These results likely indicate a Cretaceous magnetic overprint on Permian rocks. Roberts et al. (2012) analyzed a pilot sample of Galula Formation sandstones from the uppermost part of the formation while developing the magnetostratigraphy for the overlying Nsungwe Formation. Results from that work showed that thermal demagnetization procedures were successful at isolating a ChRM in the Galula Formation and that magnetostrigraphy could provide a means of further constraining the age of the Galula Formation, thus providing motivation for the current study.

The majority of paleomagnetic results from the Cretaceous of mainland Africa come from isolated igneous units, including several Late Cretaceous kimberlites from southern Africa (Mcfadden and Jones, 1977; Ito et al., 1978; Hargraves and Onstott, 1980; Hargraves, 1989; Fontana et al., 2011), the Lower Cretaceous Lupata volcanic

series of Mozambique (Gough and Opdyke, 1963) and the Wadi Natash volcanics of Egypt (Schult et al., 1981). Additional units include Lower Cretaceous exposures in Namibia and Angola associated with the Paraná-Etendeka igneous province (Gidskehaug et al., 1975; Dodd et al., 2015) and the northern volcanic field of Sudan (Saradeth et al., 1987). These results, in addition to several Upper Cretaceous volcanics from Madagascar (rotated relative to southern Africa) have been used to construct an apparent polar wander path (APWP) for the African continent through the Cretaceous (Besse and Courtillot, 2002) but are less useful for continent-wide correlation and age determination.

Far fewer paleomagnetic studies have focused on sedimentary units from the Cretaceous of Africa. The most extensively studied of these are the Upper Cretaceous Nubian Sandstone of Egypt (El Shazly and Krs, 1973; Schult et al., 1978, 1981; Hussain and Aziz, 1983; Odah, 2004) and the Lower Cretaceous "Infracenomanian sandstones" of central Morocco (Hailwood, 1975; Martin et al., 1978). Paleomagnetic studies focused on sedimentary rocks of southern Africa are particularly sparse, and limited to only a few samples of red siltstone collected from Mozambique and correlated to the Lupata volcanic series (Gough and Opdyke, 1963), the preliminary samples collected from the Songwe region described above (Nairn, 1964; Roberts et al., 2012) and a more detailed magnetostratigraphic study by Strganac et al. (2014) of Upper Cretaceous marine sediments from the Namib Basin of Angola.

In light of the sparse magnetostratigraphic record for the Cretaceous of Africa when compared to other continents, developing detailed magnetostratigraphy for the Galula Formation will provide an important reference frame for future

magnetostratigraphic studies in the region and a means of correlation between geographically distant locales.

3. Methods

3.1 Field Sampling

Field work for this study was completed in the southern portion of the Rukwa Rift Basin, in the Galula and Songwe regions (Fig. 1). Samples were collected from 52 sites across four exposures of the Galula Formation. Two primary sections were selected based on their important fossil contributions and stratigraphic positions spanning the oldest and youngest portions of the Galula Formation. These were the TZ-07 section (Songwe region) and the Mtuka River section (Galula region). Additional paleomagnetic samples were collected from outcrops of the Galula Formation along the Songwe River and along the Hamposia River, where the Galula Formation sits unconformably below the Utengule Member of the Nsungwe Formation and the Lake Beds succession. Four to six samples were collected as independently oriented hand-samples from each sampling site for paleomagnetic analysis. Where possible, fine-grained lithologies were targeted for paleomagnetic sampling as they preserve a higher proportion of single-domain magnetic mineral grains that carry a more stable remanent magnetization when compared to coarser, multi-domain grains (Butler and Banerjee, 1975). The general bedding attitude was also measured to allow for structural corrections.

The TZ-07 section was measured using a Jacob's staff and paleomagnetic sample sites were then referenced to the section measured by Roberts et al. (2004).

Paleomagnetic sample sites from the Mtuka River were referenced to the section measured and illustrated by Roberts et al. (2010) using GPS coordinates and physical landmarks.

3.2 Laboratory Processing

Three paleomagnetic samples from each site were cut into 8 cm³ cubes and these samples were subjected to stepwise thermal demagnetization procedures (between 25° — 690 °C) using an ASC Model TD-48 SC thermal demagnetizer to isolate the characteristic remanent magnetization (ChRM). Sample magnetization was measured using a 2G 755 4K Superconducting Rock Magnetometer in a three dimensional DC coil low field cage in the University of New Hampshire Paleomagnetism Laboratory and using the CryoMag paleomagnetic software package (Wack, 2010). Following demagnetization, samples were analyzed using the PuffinPlot paleomagnetic data analysis program (Lurcock and Wilson, 2012) and mean ChRM directions and associated Fisher statistics were calculated for each site. An unanchored principal component analysis (PCA) was used to define a best-fit line through demagnetization steps trending towards the origin to identify the ChRM (Kirschvink, 1980). The maximum angular deviation (MAD) was calculated for the ChRM of each sample and only samples with a MAD less than 15° were included in the study. Some samples with a ChRM suggesting reversed polarity did not show final demagnetization steps with a clear trend towards the origin, but did display an intermediate temperature component clearly following a great circle path toward a south and down direction. For these samples, a

great circle was fit through the points that characterized the southward movement and the site mean direction was determined either by the intersection of the great circles, or by calculating the Fisher mean of the great circle intersection and any PCA directions from the site (McFadden and McElhinny, 1988). A third class of samples did not show clear demagnetization towards the origin and did not follow a great circle path. Rather, demagnetization steps converged on a point somewhat away from the origin. For these sites, a Fisher mean was used to characterize the ChRM. A fourth class of samples displayed demagnetization behavior that was too unstable to interpret reliably and were excluded from further analyses.

Sites characterized entirely by PCA defined ChRM directions are considered the most reliable alpha (α) sites whereas those sites that included great circle directions or Fisher means were treated as less reliable beta (β) sites. Sites that did not pass the Watson (1956) test for randomness were excluded from the study. A fourth sample was analyzed from sites that had one or more samples with ambiguous or unresolved ChRM directions to help elucidate the site polarity. Additional calculations, including determinations of virtual geomagnetic pole (VGP) and paleomagnetic pole positions, in addition to reversal and fold tests for paleomagnetic stability were performed using the PmagPy software package (Tauxe, 2011).

In order to better understand the mineralogy controlling magnetic remanence of the Galula Formation, samples from 15 sites were selected to undergo isothermal remanent magnetization (IRM) experiments. These samples were selected to encompass the full range of observed lithologies and demagnetization patterns and included samples from each of the Galula Formation exposures sampled in this study.

IRM samples were cut into 1 cm³ cubes and subjected to increasing magnetic field intensities between 0 – 1.1 T using an ASC IM10 impulse magnet. A maximum field of 1.1 T was then applied to the x-axis of the sample, 0.4 T to the y-axis, and 0.12 T to the z-axis, following the procedure of Lowrie (1990). In doing so, magnetic moments of those mineral grains with the highest coercivity (between 0.4 T and 1.1 T) were oriented along the x-axis and the moments of minerals with the lowest coercivity (below 0.12 T) were oriented along the z-axis, with moments of intermediate coercivity grains oriented in the y direction. Samples subsequently underwent stepwise thermal demagnetization using the following temperature steps: 25, 100, 125, 150, 200, 300, 400, 500, 540, 560, 580, 610, 625, 655 and 690 °C, and the magnetic intensity for each axis was examined separately. The demagnetization pattern, together with the maximum unblocking temperatures were then used to infer the magnetic mineralogy. Minerals such as magnetite and maghemite are characterized by their low coercivities and intermediate unblocking temperatures, while hematite and goethite can be identified by their high coercivity (in excess of 1.1 T) (Lowrie, 1990). Hematite and goethite can be further distinguished from each other by their maximum unblocking temperatures (~120 °C for goethite and ~680 °C for hematite) (Lowrie, 1990). The grain size and composition of the magnetic mineral assemblages, as determined from the IRM experiments, can help to reconstruct the timing and geological setting that the ChRM was acquired.

4. Results

4.1 Isothermal Remanent Magnetization (IRM) Experiments

IRM acquisition curves (Fig. 2) reveal that Galula Formation samples do not become fully saturated, even when exposed to magnetic fields up to 1.1 T. This is characteristic of samples dominated by hematite, but may also be indicative of other high coercivity minerals like ferromagnetic goethite (Lowrie, 1990). Samples from TZ-07 differ from other exposures in having a more shallowly sloping acquisition curve under lower applied magnetic fields (less than ~0.5 T), and likely contain a smaller proportion of low coercivity minerals such as detrital magnetite, maghemite, or multidomain hematite when compared to the Mtuka section, Hamposia section, and Galula Formation – Nsungwe Formation contact site locations (Fig. 2).

Stepwise demagnetization of acquired IRM (Fig. 3) supports the prevalence of hematite in all samples, as seen by complete demagnetization at temperatures close to 690 °C. Samples from the TZ-07 section generally show a large proportion of high coercivity minerals. Here, the hard axis (x-axis) consistently makes up the largest proportion of the IRM. Samples from TZ-07 do vary in their demagnetization patterns, however, with some samples showing a relatively consistent decrease in magnetization intensity until ~690 °C (e.g., RB1404, RB1411, and RB1422), whereas sample RB1407 shows a pronounced drop in magnetization intensity occurring between ~500 and 600 °C. This change in slope is consistent with a small amount of magnetite. Samples from the Mtuka section, Hamposia section, and Galula Fm. – Nsungwe Fm. contact site show a greater variety of demagnetization trends, with some samples showing a larger proportion of low coercivity (e.g., RB1431) or intermediate coercivity minerals (e.g., RB1435 and RB1445). A similar sharp change in magnetization intensity observed at

~580 °C suggests that magnetite may be present in small amounts in each of the four exposures sampled.

4.2 Thermal Demagnetization

In general, paleomagnetic samples from the Galula Formation become fully demagnetized at temperatures approaching 690 °C (Supplemental Material). Most samples preserve three components of natural remanent magnetization (NRM). These include a very weak viscous overprint component that is removed between 0 and 100 °C, an intermediate component that is stable between 100 and approximately 600 °C as well as a ChRM component that is stable above 600 °C. Representative vector end point diagrams, equal area projections, and intensity plots displaying demagnetization patterns are shown in Figures 4 and 5.

Of the 102 samples analyzed from 31 sites in the Namba Member, 81 samples displayed clear demagnetization patterns above 600 °C with a ChRM direction that could be characterized by fitting a line through high temperature points trending towards the origin (PCA). Twelve samples showed an intermediate component whose points followed a great circle path that was used to identify the ChRM (GC) and six samples were characterized by taking a Fisher mean of the final demagnetization step directions. Three samples were excluded from study, either because they were potentially misoriented during the collection process (n = 2) or displayed ambiguous or unresolved polarity (n = 1) (Supplemental Material).

Seventy-five samples from 21 sites were examined from the Mtuka Member. Of these, 53 samples were characterized using PCA and 17 were characterized using Fisher means. No samples from the Mtuka Member were interpreted using great circles and five samples were not evaluated due to their ambiguous demagnetization patterns (Supplemental Material).

4.3 Site Calculations and Polarity Determination

Out of the 31 sites sampled from the Namba Member, 24 were alpha level sites and four were beta level sites. Three sites did not pass the Watson test for randomness at the 95% confidence level and were excluded from site-level analyses (Supplemental Material). Three sites, all from the TZ-07 locality, clearly preserved a stable, high temperature reversed component (Fig. 6A). This reversed component was identified in each of the four samples measured from the three sites, along with a strong normal overprint. Consequently, these sites were considered to represent reversed periods in the geomagnetic field when the rocks were initially magnetized. One site (RB1409) yielded a mixed polarity, with individual samples providing conflicting polarity determinations. Although this site did not pass the Watson test and was excluded from further analysis, it is worth noting that it occurred immediately above one of the reversed sites, potentially recording instability in the magnetic field during a reversal. Alpha and beta level sites together from the Namba Member yield a mean declination and inclination of 352.2°/-33.2° when tectonic corrections are applied to the bedding and the reversed site directions are inverted (Fig. 6A).

Of the 21 sample sites in the Mtuka Member, 11 were alpha level sites, two were beta level sites and eight sites were unusable, either because they failed the Watson test or because fewer than three samples from the site yielded reliable information (Supplemental Material). The Mtuka Member did not preserve any clearly reversed sites, although there were a number of sites with mixed polarity. These sites did not pass the Watson test and were excluded from further study. Alpha and beta level sites from the Mtuka Member yield a mean declination and inclination of 359.5°/-46.2° after applying tectonic corrections (Fig. 6B).

4.4 Tests for Paleomagnetic Stability

Alpha level sites (n = 24) from the Namba Member passed the fold test (Tauxe and Watson, 1994), and display maximum clustering of directions between 47 – 104% untilting, consistent with a prefolding magnetization (Supplemental Material). Sites from the Mtuka Member do not display adequate variation in bedding attitude to apply the fold test, and the test is therefore not statistically powerful enough for constraining the timing of magnetization.

A parametric bootstrap reversal test (Tauxe et al., 2016) was also applied to the Namba Member as this is the only portion of the Galula Formation that preserves reversed polarity sites. When the mean direction of the reversed polarity sites (n = 3) is inverted, the 95% confidence interval overlaps with that of the normal polarity sites (n = 25) in each Cartesian direction, indicating that these populations are not significantly

different (Supplemental Material). The small reversed population size, however, makes this test somewhat weak.

4.5 Magnetic Reversal Stratigraphy

A revised stratigraphic section for the TZ-07 locality measured by Roberts et al. (2004) includes approximately 140 m of sediment associated with the Namba Member. Paleomagnetic sample sites for this study were collected through the lower 105 m, as the uppermost portion of the section was characterized by heavy vegetation cover and deep weathering. Each of the short reversed intervals from the TZ-07 section is represented by only one sampling site (Fig. 7). One of these sites occurs in the lower middle portion of the section (approximately 33 m) whereas the other two reversed intervals are located near the top of the sampled section (94 m and 104 m). Additional paleomagnetic samples were collected from sites immediately surrounding the reversed intervals during a second field season and confirmed the short duration of these intervals by having normal polarity adjacent to the reversed sections.

The original stratigraphic section measured from the Mtuka River section (Roberts et al., 2010) includes approximately 160 m of relatively continuous exposures of the Mtuka Member and approximately 350 m of relatively discontinuous exposures of the Namba Member. Paleomagnetic samples were collected through the entire Mtuka Member, as well as the lowermost ~50 m of the Namba Member (Fig. 8). The Mtuka and Namba members are both characterized by a dominant normal polarity, with

ambiguous mixed polarity sites (described above) found throughout the section in both members.

Paleomagnetic sample sites from the Hamposia and Songwe Rivers display entirely normal polarity and lack the mixed polarity signals that characterize the Mtuka River section.

4.6 Paleomagnetic Pole

Paleomagnetic poles calculated from alpha level sites in the Namba (246.4°/77.9°, α₉₅ 5.9°) and Mtuka (217.1°/ 72.2°, α₉₅ 11.1°) members overlap with the Late Cretaceous apparent polar wander path (APWP) for Africa and are most similar to the poles from the 60 – 70 Ma age range (Fig. 9; Besse and Courtillot, 2003; Torsvik et al., 2012). It should be noted, however, that there is considerable overlap with a wide range in ages between 100 Ma and 30 Ma. Red beds, such as the Galula Formation, are particularly susceptible to inclination shallowing during deposition, potentially leading to offset between their observed inclination and that predicted from their paleolatitude (Tauxe and Kent, 2004). We corrected for inclination shallowing using a flattening factor of f = 0.6 on site mean directions from the Namba and Mtuka members, following the procedure of Tauxe and Kent (2004), to test whether this would improve the fit of our calculated paleomagnetic poles with the African APWP. The corrected poles do not consistently align more closely with the published APWPs or change our preferred correlation and we therefore use the uncorrected poles in this paper. As a whole, the paleomagnetic poles are most consistent with a Late Cretaceous age for the

Namba and Mtuka members, an estimate that is somewhat younger, but not inconsistent, with previous age estimates based on biostratigraphy and regional geology (see Section 2.1.3).

5. Discussion

5.1 Correlation to the Geomagnetic Polarity Timescale (GPTS)

The relatively long (~150 m) exposure of the Mtuka Member sampled for this study preserves dominantly normal polarity throughout, and is consistent with deposition during the CNS, between approximately 121 Ma and 83 Ma. Sedimentological evidence, however, supports a relatively slow generation of accommodation space and sediment deposition for the Galula Formation (Roberts et al., 2010), a characteristic that increases the chance of missing a reversed interval in a sampling gap. The vertebrate fauna from the Mtuka Member is equivocal in terms of constraining the age of this member further, however it is generally consistent with deposition during the CNS in the middle Cretaceous. Further refinement of the fauna or discovery of datable volcanic material will be necessary for a more precise age.

Another notable feature of the paleomagnetic record from the Mtuka Member is the prevalence of sites with samples showing conflicting polarity. It is possible that this reflects instability in the geomagnetic field at this time; however, the demagnetization of acquired IRM suggests that a combination of high and low coercivity magnetic minerals over a range of grain sizes are present, indicating that variable lithology may play a

larger role in the heterogeneity of paleomagnetic results from the Mtuka Member.

Alternatively, these results could indicate variable degrees of later remagnetization or magnetic overprinting in the Mtuka Member, something that is less pronounced in Namba Member samples from the Hamposia section, TZ-07 and the Galula Formation – Nsungwe Formation contact site. Similar lithological influence on paleomagnetic behavior has been documented in other portions of the CNS (e.g., Cronin et al., 2001) and proposed as a counterargument to suggested excursionary behavior during this interval.

Despite having a better understood, and potentially more temporally diagnostic vertebrate fauna, the Namba Member correlation to the GPTS is more uncertain than the Mtuka Member. Assuming the three, short-duration reversed periods near the top of the unit are indeed representative of magnetic field reversals (an assumption that is supported by having four consistently reversed samples from each site), a logical correlation would be to the three short reversed periods in Chron C32 (Fig. 10A). This correlation would place the TZ-07 fossil localities in the upper Campanian or lowermost Maastrichtian. This correlation is compatible with the known vertebrate fauna, particularly given the occurrence of a gondwanatherian mammal, a group whose currently known range begins in the Campanian.

The paleomagnetic poles calculated for the Galula Formation (this study) are also consistent with a Late Cretaceous age (Cenomanian or younger; Fig. 9).

Geological age constraints, however, are less supportive of a Campanian age for the Galula Formation, and rather suggest a middle Cretaceous age for at least part of the unit (Fig. 11). The age of emplacement (~119 – 96 Ma) for regional carbonatite found to

cross-cut red beds presumably associated with the Galula Formation (Fawley and James, 1955; Roberts et al., 2010), is generally consistent with age estimates based on the seismic velocity – depth relationship (Faust, 1951; Mliga, 1994), maximum age estimates for the TZ-07 locality (Namba Member) based on detrital zircons (Fig. 11) and contemporaneous deposition with the Aptian Malawi Dinosaur Beds. Together, these point to an Aptian – Cenomanian age, though it remains unclear how the individual members of the Galula Formation fit into this age framework. Moreover, recent uncertainty surrounding the age of the Panda Hill Carbonatite (see Section 2.1.2 for discussion) complicates its use as a significant age constraint for the formation.

If the Namba Member is Campanian in age as suggested by this paleomagnetic correlation, its deposition could be associated with continent-wide tectonic activity during the Late Cretaceous. Changing seafloor-spreading configurations in the southern and central Atlantic Ocean basins during this time correspond to the development of compressional and shearing forces with associated sedimentation in the West and Central African Rift Zones (Fairhead, 1988; Fairhead and Binks, 1991; Binks and Fairhead, 1992). Apatite fission track analysis paired with numerical thermal modelling from northern Namibia also reveal a period of cooling and denudation beginning at approximately 70 Ma in southern Africa, postdating the initial opening of the Atlantic ocean at approximately 130 Ma (Brown et al., 2014). There is also evidence for rifting initiating in eastern Africa in the Anza Basin of Kenya during the Cenomanian and continuing through the Maastrichtian (Bosworth and Morley, 1994). Under this scenario, deposition of the Namba Member could be contemporaneous with formation of the

Lapurr Sandstones of Kenya, interpreted to be Turonian – Campanian and associated with the initiation of rifting in the Anza Basin (O'Connor et al., 2011).

An alternative correlation would assign one of the TZ-07 reversals to C33r, an approximately 4 myr reversed period at the base of the Campanian (Ogg and Hinnov, 2012). This correlation would give a pre-Campanian age to fossils at the TZ-07 locality. This interpretation is difficult to reconcile with the span of time (3.74 myr) that would be represented by the short reversals in this part of the section. Sedimentation rates calculated for each of the reversed intervals, assuming correlation to Chron C33r, are two orders of magnitude lower than what is expected for fluvial environments in general (Sadler, 1981), whereas rates calculated for the C32 reversals are consistent with observed values. Additionally, there are no well-documented reversals close to C33r that would correlate to the other two reversals at TZ-07. This correlation is therefore not favored.

A third interpretation that deserves consideration is that these reversals represent short reversed periods during the CNS (Fig. 10B) The observation of short magnetically-reversed intervals during this presumably stable time for Earth's geomagnetic field has recently gained attention in the literature as the result of more detailed magnetostratigraphic investigations from marine sediments (Ryan et al., 1978; Hailwood, 1979; Tarduno, 1990; Ogg and Hinnov, 2012). Seafloor sediment cores support the presence of a short reversed period stratigraphically above Chron M0r and within the narrowly defined *Globigerinelloides alergerianus* biostratigraphic zone (middle Aptian) (Tarduno, 1990). This reversed period, variably referred to as "ISEA" or Chron M -1r, is estimated to represent only approximately 100 kyr (Hailwood, 1979, Tarduno

1990), possibly accounting for its absence in the seafloor magnetic anomaly record. Subsequent work in the Albian Contessa Section of Italy as well as additional seafloor drilling revealed support for two additional reversed intervals during the Albian (Chrons M -2r and M -3r) and strengthens the argument for short magnetic reversals during the CNS (Keating and Helsley, 1978; Hailwood, 1979; Tarduno et al., 1992; Ogg and Hinnov, 2012), although it has been proposed that these may merely reflect reversed magnetic overprints imposed during Chron C33r (Tarduno et al., 1992).

Magnetostratigraphic studies focused on constraining the end of the CNS, have also found reversed intervals stratigraphically below C33r. A high resolution, geochronologic and magnetostratigraphic investigation of the Songliao Basin, China (He et al., 2012; Wang et al., 2016) found three short reversed intervals near the end of the superchron (early Santonian, ~85 Ma). Work focused on the Coniacian – Campanian chalk sequences of England found predominantly reversed layers in the Campanian portion of the section, with multiple short reversals during the Coniacian – Santonian leading up to the end of the CNS (Montgomery et al., 1998), a finding that is supported by study of Cenomanian – Campanian deposits of Turkmenistan (Guzhikov et al., 2003).

Although there is no strong consensus concerning the precise timing for reversals during the CNS, there is growing support for their existence. Most evidence supports three short reversals during the Aptian – Albian (M -1r, M -2r, and M -3r) (Ogg and Hinnov, 2012) as well as a mixed polarity interval later in the CNS (Cenomanian – Santonian). The short duration of these reversed periods, as well as the temporal overlap with several lines of faunal and geological age constraints make these a

reasonable interpretation for reversals in the Namba Member, particularly reversals near the end of the CNS. We consider this as an alternative correlation for the Namba Member, with a preferred correlation for the Namba Member being Chron C32. Final resolution of these competing correlations for the Galula Formation will require the application of additional chronostratigraphic methods to further constrain its age.

5.2 Correlation to the Malawi Dinosaur Beds

The Cretaceous Dinosaur Beds of Malawi (Jacobs et al., 1990) are thought to overlap in time, at least partially, with the Galula Formation and are considered to be one of its best analogs. These beds occur in the Malawi Rift, a continuation of the Western Branch of the East African Rift System, approximately 200 km southeast of the Galula Formation exposures. The Dinosaur Beds are lithologically varied, with a lower member comprised of deep red stained sandstones that lacks fossils, and an upper, fossil-rich member comprised of white sands and grey to red mudstones and siltstones (Jacobs et al., 1990). Several vertebrate taxa have been recognized from the Malawi Dinosaur Beds, including two species of osteichthyans, two anurans, a pelomedusid turtle, notosuchian and non-notosuchian crocodyliforms, as well as non-avian theropods and titanosaurian sauropods (Jacobs et al., 1990; Gomani, 1997, 2005).

The Malawi Dinosaur Beds have traditionally been assigned an Aptian age, based on the vertebrate fauna as well as a lacustrine ostracod assemblage. The ostracods are assigned to the family Cyprididae, and tentatively to the genus *Horcquia* (Colin and Jacobs, 1990). This genus is known from primarily Aptian deposits in

western Africa and South America, and constrain the age of the Dinosaur Beds to Late Jurassic – Aptian, with strongest support for a Barremanian – Aptian age (Colin and Jacobs, 1990). Faunal comparisons with other African vertebrate localities suggest the Malawi Dinosaur Beds are younger than the Jurassic Tendaguru Beds of Tanzania, and more similar to the Lower Cretaceous (~Aptian) units of western Africa, including the Gadoufaoua locality in Niger and the Koum Basin, Cameroon (Jacobs et al., 1990). These localities, however, are imprecisely dated, with Gadoufaoua having only a minimum age constraint from overlying Cenomanian marine beds (Taquet, 1976) and a fauna that is generally consistent with an Early Cretaceous age. The Koum Basin is less constrained and merely correlated to Gadoufaoua based on general faunal similarities.

Like the Galula Formation, the Malawi Dinosaur Beds lack rigorous age constraint from radiometric dating, and similarly, no primary volcanic material has been recovered from these beds to help resolve this issue. Furthermore, no magnetostratigraphic study of the Dinosaur Beds has been conducted to support the Aptian age assignment or provide a means to correlate with the Galula Formation. The uncertainty surrounding these ages and correlations with other African Cretaceous faunas and rock units highlights the need for additional work before the Galula Formation and Dinosaur Beds can be confidently placed within a regional, continental, and global context.

Titanosaurian sauropods are a conspicuous element of both the Galula

Formation (Namba Member) and the Malawi Dinosaur Bed faunas. However, recent
analyses have not identified close relationships among these forms (Gorscak and
O'Connor, 2016; Gorscak et al., 2017). Also, both the Namba Member and the Malawi

Dinosaur Beds preserve notosuchian crocodyliforms, a group that has thus far not been recovered from the lower Mtuka Member. Nonetheless, the putative Aptian age for the Dinosaur Beds and a similar age assessment of the Mtuka Member as presented herein suggests a potential correlation for these two units. Ongoing faunal analyses based on materials (e.g., an undescribed titanosaurian sauropod) recovered from the Mtuka Member of the Galula Formation may directly address this point. Finally, a correlative relationship between the Mtuka Member and the Malawi Dinosaur Beds also supports the interpretation that the Namba Member and its associated fauna is younger than that of the Malawi Dinosaur Beds, minimally consistent with the observation noted above about the distinct dinosaurian faunas in the two units.

5.3 Cretaceous Paleobiogeography Implications

Both magnetostratigraphic correlations supported by this study suggest deposition of the Namba Member occurred after 100 Ma, and minimally allow us to constrain the timing of deposition to Cenomanian – Campanian (Fig. 10). All models for the breakup of Gondwana suggest that continental Africa should be isolated from other continents by this time. The vertebrate fauna from the Namba Member remains generally similar to other Late Cretaceous Gondwanan locales. At a higher degree of examination, previous faunal comparisons using sauropod dinosaurs and mammal-like notosuchian crocodyliforms from Tanzania and Malawi with those from circum-Saharan localities suggested that the southern representatives of these groups are more similar to each other than to their northern counterparts (Gomani, 2005; O'Connor et al., 2010;

Gorscak et al., 2014, 2017; Sertich and O'Connor, 2014), supporting the notion of faunal provinciality in Africa during the Cretaceous. This pattern may also be present in African lungfishes, with the Galula Formation *Lupaceratodus useviaensis* (Gottfried et al., 2009) possessing several characteristics not exhibited by forms known from northern Africa. In contrast, the Namba Member peirosaurid *Rukwasuchus yajabalijekundu* (Sertich and O'Connor, 2014) closely resembles middle – Late Cretaceous crocodyliforms known from circum-Saharan Africa, including *Stolokrosuchus lapparenti* and *Hamadasuchus rebouli* and expands the previously known range for this group into southern Africa. The peirosaurid from Tanzania, therefore, provides some of the strongest evidence for a more widespread distribution for certain clades across the African Continent during the Cretaceous, with future fossil discoveries from southern Africa being critical to further assess the generality of such patterns.

The Mtuka Member is likely Aptian – Cenomanian given its normal polarity and stratigraphic position below the Namba Member (Fig. 10). Until the Mtuka fauna is developed further, it has little utility for evaluating the existing paleobiogeographic hypotheses. The Early – middle Cretaceous age of this member, however, places it in an important position to potentially test these hypotheses as the fauna becomes better understood. Under each of the paleobiogeographic hypotheses, the Aptian – Albian faunas of continental Africa are predicted to be similar to other Gondwanan landmasses with the faunas beginning to diverge either before ("Africa First" hypothesis) or after ("Pan-Gondwana" hypothesis) the Albian – Cenomanian transition

6. Conclusions

Using magnetostratigraphy to constrain the timing of deposition for the Galula Formation, we find that the upper Namba Member is characterized by three short magnetic reversals near the top of the section. We propose two potential correlations for relating these reversals to the GPTS, with the first one favored here: (1) These reversals may be equivalent to Chron C32 (Campanian), or (2) the reversals may represent short excursions during the upper part of the CNS (C34n). Together these interpretations constrain the age of the Namba Member to Cenomanian – Campanian, a significant refinement over previous constraints. The underlying Mtuka Member is dominated by normal polarity, consistent with deposition in the lower portion of the CNS (Aptian – Cenomanian). The paleomagnetic poles calculated for the Namba $(246.4^{\circ}/77.9^{\circ}, \alpha_{95} 5.9^{\circ})$ and Mtuka $(217.1^{\circ}/72.2^{\circ}, \alpha_{95} 11.1^{\circ})$ members are also most consistent with a Late Cretaceous (Cenomanian or younger) age.

These results provide important new constraints on the age of the paleontologically important Galula Formation and will facilitate correlation to other African units as their magnetostratigraphy (and age constraint more generally) becomes better developed. Additional chronostratigraphic work is needed in the Rukwa Rift and other African vertebrate-bearing locales to understand the vertebrate faunas from the Galula Formation in the context of competing paleobiogeographic hypotheses and to understand the relationship between the Galula fauna and those of other Gondwanan regions.

Acknowledgements

Funding was provided by NSF (EAR 1349825 to P.M.O. and EAR 1349592 to W.C.C.) as well as a Geological Society of America Graduate Student Research Grant and University of New Hampshire, Dept. of Earth Sciences Graduate Student Research Grant to S.J.W. The funding sources were not involved in the study design, data collection or interpretation, or publication.

We would like to thank the Antiquities Unit of the Tanzanian Ministry of Natural Resources and Tourism and the Tanzanian Commission for Science and Technology (COSTECH) for logistical help coordinating field research and the Utengule Coffee Lodge (Mbeya, Tanzania) for their hospitality during field work. Additionally we would like to thank the 2014 and 2015 field team participants (Eric Gorscak, Hannah Hilbert-Wolf, Waymon Holloway, Zubair Jinnah, Cassy Mtelela, Emily Naylor and the late Joseph Temu) for assistance in the field and Joel Johnson and Eric Gorscak for helpful comments on the manuscript. C. Mac Niocaill and one anonymous reviewer are thanked for comments on the initial submission of this paper.

References

Ali, J.R., Krause, D.W., 2011. Late Cretaceous bioconnections between Indo-Madagascar and Antarctica: Refutation of the Gunnerus Ridge causeway hypothesis. J. Biogeogr. 38, 1855–1872. doi:10.1111/j.1365-2699.2011.02546.x Besse, J., Courtillot, V., 2002. Apparent and true polar wander and the geometry of the

- geomagnetic field over the last 200 Myr. J. Geophys. Res. 107. doi:10.1029/2003JB002684
- Besse, J., Courtillot, V., 2003. Correction to "Apparent and true polar wander and the geometry of the geomagnetic field over the last 200 Myr." J. Geophys. Res. 108, 9–10. doi:10.1029/2003JB002684
- Binks, R. M., and J. D. Fairhead. 1992. A plate tectonic setting for Mesozoic rifts of West and Central Africa. Tectonophysics 213:141–151.
- Bonaparte, J.F., Novas, F.E., 1985. *Abelisaurus Comahuensis*, N. G., N. Sp.,

 Carnosauria from the Late Cretaceous of Patagonia. Ameghiniana 21, 259–265.
- Bosworth, W., and C. K. Morley. 1994. Structural and stratigraphic evolution of the Anza rift, Kenya. Tectonophysics 236:93–115.
- Brown, R., M. Summerfield, A. Gleadow, K. Gallagher, A. Carter, R. Beucher, and M. Wildman. 2014. Intracontinental deformation in southern Africa during the Late Cretaceous. Journal of African Earth Science 100:20–41.
- Butler, R.F., Banerjee, S.K., 1975. Theoretical single-domain grain size range in magnetite and titanomagnetite. J. Geophys. Res. 80. 4049–4058. DOI: 10.1029/JB080i029p04049
- Channell, J.E.T., Erba, E., Nakanishi, M., Tamaki, K., 1995. Late Jurassic-Early

 Cretaceous time scales and oceanic magnetic anomaly block models.

 Geochronology, Time Scales Glob. Stratigr. Correl. SEPM Spec. Publ. 51–64.
- Choh, A.M., 2007. Palaeoenvironment and palaeoclimate of the Red Sandstone Group

- in the Rukwa Rift Basin, Tanzania. Unpublished honors thesis. University of the Witwatersrand, Johannesburg, 51 p.
- Chorowicz, J., 2005. The East African rift system. J. African Earth Sci. 43, 379–410. doi:10.1016/j.jafrearsci.2005.07.019
- Coffin, M.F., Rabinowitz, P.D., 1988. Evolution of the conjugate East African Madagascan margins and the western Somali Basin. Geol. Soc. Am. Spec. Pap.
 226, 1–79. doi:10.1130/SPE226-p1
- Colin, J.K., Jacobs, L., 1990. On the age of the Malawi Dinosaur Beds: evidence from ostracodes. Comptes Rendus l'Académie des Sci. Paris Série II 331 1025–1029.
- Cronin, M., Tauxe, L., Constable, C., Selkin, P., Pick, T., 2001. Noise in the quiet zone. Earth Planet. Sci. Lett. 190, 13–30. doi:10.1016/S0012-821X(01)00354-5
- De Klerk, W.J., Forster, C.A., Sampson, S.D., Chinsamy, A., Ross, C.F., 2000. A new coelurosaurian dinosaur from the Early Cretaceous of South Africa. J. Vertebr. Paleontol. 20, 324–332.
- Dodd, S.C., Muxworthy, A.R., Mac Niocaill, C., 2015. Paleointensity determinations from the Etendeka province, Namibia, support a low-magnetic field strength leading up to the Cretaceous normal superchron. Geochemistry, Geophys. Geosystems 16, 785–797. doi:10.1002/2014GC005707
- Eizirik, E., Murphy, W.J., O'Brien, S.J., 2001. Molecular dating and biogeography of the early placental mammal radiation. J. Hered. 92, 212–219.

 doi:10.1093/jhered/92.2.212

- El Shazly, E., Krs, M., 1973. Paleogeography and paleomagnetism of the Nubian Sandstone Eastern Desert of Egypt. Geol. Rundschau 62, 212–225.
- Ezcurra, M. D., & Agnolín, F. L., 2011. A new global palaeobiogeographical model for the Late Mesozoic and Early Tertiary. Systematic Biology, 61(4), 553-566.
- Fairhead, J. D. 1988. Mesozoic plate tectonic reconstructions of the central South

 Atlantic Ocean: The role of the West and Central African rift system.

 Tectonophysics 155:181–191.
- Fairhead, J. D., and R. M. Binks. 1991. Differential opening of the Central and South Atlantic Oceans and the opening of the West African rift system. Tectonophysics 187:191–203.
- Faust, L.Y., 1951. Seismic velocity as a function of depth and geologic time.

 Geophysics 16, 192–206. doi:10.1190/1.1437658
- Fawley, A.P., James, T.C., 1955. A pyrochlore (columbium) carbonatite, southern Tanganyika. Econ. Geol. 50, 571–585.
- Feldmann, R., O'Connor, P., Stevens, N., Gottfried, M., Roberts, E., Ngasala, S., Rasmusson, E., Kapilima, S., 2007. A new freshwater crab (Decapoda: Brachyura: Potamonautidae) from the Paleogene of Tanzania, Africa. Neues Jahrb. für Geol. und Paläontologie Abhandlungen 244, 71–78. doi:10.1127/0077-7749/2007/0244-0071
- Fontana, G., Mac Niocaill, C., Brown, R.J., Sparks, R.S.J., Field, M., 2011.

 Emplacement temperatures of pyroclastic and volcaniclastic deposits in kimberlite

- pipes in southern Africa. Bull. Volcanol. 73:1063-1083. doi: 10.1007/s00445-011-0493-9
- Friedrich, O., Norris, R.D., Erbacher, J., 2012. Evolution of middle to Late Cretaceous oceans A 55 m.y. record of Earth's temperature and carbon cycle. Geology 40, 107–110. doi:10.1130/G32701.1
- Gidskehaug, A., Creerf, K.M., Mitchell, J.G., 1975. Palaeomagnetism and K-Ar Ages of the South-west African Basalts and their bearing on the time of initial rifting of the South Atlantic Ocean. Geophys. J. R. Astron. Soc. 1–20.
- Gomani, E.M., 2005. Sauropod Dinosaurs from the Early Cretaceous of Malawi, Africa. Palaeontol. Electron. 8, 1–37.
- Gomani, E.M., 1997. A Crocodyliform from the Early Cretaceous Dinosaur Beds, Northern Malawi. J. Vertebr. Paleontol. 17, 280–294.
- Gorscak, E., O'Connor, P., Stevens, N., Roberts, E., 2014. The Basal Titanosaurian Rukwatitan Bisepultus (Dinosauria, Sauropoda) from the middle Cretaceous Galula Formation,Rukwa Rift Basin, southwestern Tanzania. J. Vertebr. Paleontol. 35, 1133–1154. doi:10.1080/02724634.2014.845568
- Gorscak, E., and P. M. O. Connor. 2016. Time-calibrated models support congruency between Cretaceous continental rifting and titanosaurian evolutionary history. Biology Letters 12.
- Gorscak, E., O'Connor, P.M., Roberts, E.M., Stevens, N.J., 2017. The second titanosaurian (Dinosauria: Sauropoda) from the middle Cretaceous Galula

- Formation, southwestern Tanzania with remarks on African titanosaurian diversity.

 Journal of Vertebrate Paleontology. 37(4) e13443250.
- Gottfried, M.D., O'Connor, P.M., Jackson, F.D., Roberts, E.M., Chami, R., 2004.

 Dinosaur eggshell from the Red Sandstone Group of Tanzania. J. Vertebr.

 Paleontol. 24, 494–497. doi:10.1671/0272-4634(2004)024[0494:DEFTRS]2.0.CO;2
- Gottfried, M.D., Stevens, N.J., Roberts, E.M., O'Connor, P.M., Chami, R., 2009. A new Cretaceous lungfish (Dipnoi: Ceratodontidae) from the Rukwa Rift Basin, Tanzania.

 African Nat. Hist. 5, 1–6.
- Gough, D.I., Opdyke, N.D., 1963. The Palaeomagnetism of the Lupata Alkaline Volcanics. Geophys. J. Int. 7. 457 468.
- Granot, R., Dyment, J., 2015. The Cretaceous opening of the South Atlantic Ocean.

 Earth Planet. Sci. Lett. 414, 156–163. doi:10.1016/j.epsl.2015.01.015
- Grantham, D.R., Teale, E.O., Spurr, A.M., Harkin, D.A., Brown, P.E., 1958. Quarter Degree Sheet 244 (Mbeya). Geol. Surv. Tanganyika, Dodoma.
- Guzhikov, A.Y., Molostovskii, E.A., Nazarov, K., Fomin, V.A., Baraboshkin, E.Y., Kopaevich, L.F., 2003. Magnetostratigraphic data on the Upper Cretaceous of Tuarkyr (Turkmenistan) and their implications for the general paleomagnetic time scale. Izv. Phys. Solid Earth 39, 728–740.
- Hailwood, E.A., 1979. Paleomagnetism of late Mesozoic to Holocene sediments from the Bay of Biscay and Rockall Plateau, drilled on IPOD Leg 48. Montadert, L., Roberts, DG, al., Init.Repts.DSDP 48, 305–339.

- Hailwood, E.A., 1975. The Palaeomagnetism of Triassic and Cretaceous Rocks from Morocco. Geophys. J. R. Astron. Soc. 219–235.
- Hargraves, R.B., 1989. Paleomagnetism of Mesozoic kimberlites in Southern Africa and the Cretaceous apparent polar wander curve for Africa. J. Geophys. Res. 94, 1851–1866.
- Hargraves, R.B., Onstott, T.C., 1980. Paleomagnetic results from some southern

 African kimberlites, and their tectonic significance. J. Geophys. Res. Solid Earth 85,

 3587–3596. doi:10.1029/JB085iB07p03587
- Hay, W.W., Deconto, R.M., Wold, C.N., Wilson, K.M., Voigt, S., Schulz, M., Wold, A.R.,
 Dullo, W.-C., Ronov, A.B., Balukhovsky, A.N., Söding, E., 1999. Alternative global
 Cretaceous paleogeography. Evol. Cretac. Ocean. Syst. Geol. Soc. Am. Spec.
 Pap. 332 1–47. doi:10.1130/0-8137-2332-9.1
- He, H., C. Deng, W. Pujun, Y. Pan, and R. Zhu. 2012. Toward age determination of the termination of the Cretaceous Normal Superchron. Geochemistry Geophysics Geosystems 13:1–20.
- Hilbert-Wolf, H.L., Roberts, E.M., Simpson, E.L., 2016. New sedimentary structures in seismites from SW Tanzania: Evaluating gas- vs. water-escape mechanisms of soft-sediment deformation. Sediment. Geol. doi:10.1016/j.sedgeo.2016.03.011
- Hussain, A.G., Aziz, Y., 1983. Paleomagnetism of Mesozoic and Tertiary rocks from East El Owenat Area, southwest, Egypt. J. Geophys. Res. Solid Earth 88, 3523–3529.

- Ito, H., Tokieda, K., Suwa, K., Kume, S., 1978. Cretaceous kimberlites in South Africa. Geophys. J. R. Astron. Soc. 55, 123–130.
- Jacobs, L.L., Winkler, D.A., Kaufulu, Z.M., Downs, W.R., 1990. The dinosaur beds of northern Malawi, Africa. Natl. Geogr. Res. 6, 196–204.
- Keating, B. H., and C. E. Helsley. 1978. Magnetostratigraphy of Cretaceous age sediments from Sites 361, 363 and 364. Bolli, HM, Ryan, WBF, et al., Init. Repts. DSDP 40:459–468.
- Kilembe, E.A., Rosendahl, B.R., 1992. Structure and stratigraphy of the Rukwa rift.

 Tectonophysics 209, 143–158.
- Kirschvink, J.L., 1980. The least-squares line and plane and the analysis of paleomagnetic data. Geophys. J. R. Astron. Soc. 62, 699–718. doi:10.1111/j.1365-246X.1980.tb02601.x
- Krause, D.W., Prasad, G.V.R., von Koenigswald, W., Sahni, A., Grine, F., 1997.

 Cosmopolitanism among Gondawanan Late Cretaceous mammals. Nature 390, 504–507. doi:10.1016/S0899-5362(98)90644-3
- Krause, D.W., Rogers, R.R., Forster, C.A., Hartman, J.H., Buckley, G.A., Sampson, S.D., 1999. The Late Cretaceous vertebrate fauna of Madagascar: Implications for Gondwanan paleobiogeography. GSA Today 9, 1–7.
- Krause, D.W., Gottfried, M.D., O Connor, P.M., Roberts, E.M., 2003. A Cretaceous mammal from Tanzania. Acta Palaeontol. Pol. 48, 321–330.
- Krause, D.W., O'Connor, P.M., Rogers, K.C., Sampson, S.D., Buckley, G. A., Rogers,

- R.R., 2006. Late Cretaceous terrestrial vertebrates from Madagascar: Implications for Latin American biogeography. Ann. Missouri Bot. Gard. 93, 178–208. doi:10.3417/0026-6493(2006)93[178:LCTVFM]2.0.CO;2
- Krause, D.W., Hoffmann, S., Wible, J.R., Kirk, E.C., Schultz, J.A., von Koenigswald, W.,
 Groenke, J.R., Rossie, J.B., O'Connor, P.M., Seiffert, E.R., Dumont, E.R.,
 Holloway, W.L., Rogers, R.R., Rahantarisoa, L.J., Kemp, A.D., Andriamialison, H.,
 2014. First cranial remains of a gondwanatherian mammal reveal remarkable
 mosaicism. Nature 515, 512–517. doi:10.1038/nature13922
- Lawver, L.A., Gahagan, L.M., Coffin, M.F., 1992. The development of paleoseaways around Antarctica, in: The Antarctic Paleoenvironment: A Perspective on Global Change: Part One. Antarctic Research Series, 56, 7–30.
- Le Loeuff, J., Läng, E., Cavin, L., Buffetaut, E., 2012. Between Tendaguru and Bahariya: On the age of the Early Cretaceous dinosaur sites from the Continental Intercalaire and other African formations. Journal of Stratigraphy, 36(2).
- Longrich, N. R., Pereda-Suberbiola, X., Jalil, N. E., Khaldoune, F., & Jourani, E., 2017.

 An abelisaurid from the latest Cretaceous (late Maastrichtian) of Morocco, North

 Africa. Cretaceous Research, 76, 40-52.
- Lowrie, W., 1990. Identification of ferromagnetic minerals in a rock by coercivity and unblocking temperature properties. Geophys. Res. Lett. 17, 159–162.
- Lurcock, P.C., Wilson, G.S., 2012. PuffinPlot: A versatile, user-friendly program for paleomagnetic analysis. Geochemistry, Geophys. Geosystems 13, 1–6. doi:10.1029/2012GC004098

- Maisey, J.G., 2000. Continental break up and the distribution of fishes of Western Gondwana during the early Cretaceous. J. African Earth Sci. 21, 281 314. doi:10.1016/S0899-5362(01)80081-6
- Martin, D.L., Nairn, A.E.M., Noltimier, H.C., Petty, M.H., Schmitt, T.J., 1978. Paleozoic and Mesozoic paleomagnetic results from Morocco. Tectonophysics 44, 91–114.
- Mateus, O., Jacobs, L.L., Schulp, A.S, Polcyn, M.J., Tavares, T.S., Neto, A.B., Morais,
 M.L., Antunes, M.T., 2011. *Angolatitan adamastor*, a new sauropod dinosaur and
 the first record from Angola. Annals of the Brazilian Academy of Sciences, 83(1):
 221-233.
- Mcfadden, P.L., Jones, D.L., 1977. The palaeomagnetism of some Upper Cretaceous kimberlite occurrences in South Africa. Earth Planet. Sci. Lett. 34, 125–135.
- McFadden, P.L., McElhinny, M., 1988. The combined analysis of remagnetisation circles and direct observation in palaeomagnetism. Earth Planet. Sci. Lett. 87, 161–172.
- McKinlay, A.C.M., 1965. The coalfields and the coal resources of Tanzania. Tanganyika Geol. Surv. Bull., 38.
- Mesko, G.T., Class, C., Magway, M.D., Boniface, N., Manya, S., Hemming, S.R., 2014.

 The timing of early magmatism and extension in the southern East African Rift:

 tracking geochemical source variability with 40 Ar / 39 Ar geochronology at the

 Rungwe volcanic province, SW Tanzania, in: American Geophysical Union, Fall

 Meeting, Abstract.

- Mliga, N.R., 1994. Depositional environments, stratigraphy and hydrocarbon potential of the Rukwa Rift Basin–SW Tanzania. Duke University. Doctoral Dissertation.
- Montgomery, P., Hailwood, E.A., Gale, A.S., Burnett, J.A., 1998. The magnetostratigraphy of Coniacian-Late Campanian chalk sequences in southern England. Earth Planet. Sci. Lett. 156, 209–224. doi:http://dx.doi.org/10.1016/S0012-821X(98)00008-9
- Morley, C.K., Cunningham, S.M., Harper, R.M., Wescott, W.A., 1999. Geology and Geophysics of the Rukwa Rift, East Africa, in: Morley, C.K. (Ed.), Geoscience of Rift Systems Evolution of East Africa. Tulsa, pp. 91–110.
- Murphy, W.J., Eizirik, E., O'Brien, S.J., Madsen, O., Scally, M., Douady, C.J., Teeling,
 E., Ryder, O. A., Stanhope, M.J., de Jong, W.W., Springer, M.S., 2001. Resolution of the early placental mammal radiation using Bayesian phylogenetics. Science 294, 2348–2351. doi:10.1126/science.1067179
- Nairn, A.E.M., 1964. Palaeomagnetic measurements on Karroo and post-Karroo rocks.

 A second progress report. Overseas Geol. Miner. Resour. Gt. Britain 9, 302–320.
- Néraudeau, D., Mathey, B., 2000. Biogeography and diversity of South Atlantic

 Cretaceous echinoids: Implications for circulation patterns. Palaeogeogr.

 Palaeoclimatol. Palaeoecol. 156, 71–88. doi:10.1016/S0031-0182(99)00132-7
- Nyblade, A.A., Lei, Y., Shive, P.N., Tesha, A., 1993. Paleomagnetism of Permian sedimentary rocks from Tanzania and the Permian paleogeography of Pangea. Earth Planet. Sci. Lett. 118, 181–194. doi:10.1016/0012-821X(93)90167-8

- O'Connor, P.M., Gottfried, M.D., Stevens, N.J., Roberts, E.M., Ngasala, S., Kapilima, S., Chami, R., 2006. A new vertebrate fauna from the Cretaceous Red Sandstone Group, Rukwa Rift Basin, Southwestern Tanzania. J. African Earth Sci. 44, 277–288. doi:10.1016/j.jafrearsci.2005.11.022
- O'Connor, P.M., Sertich, J.J.W., Stevens, N.J., Roberts, E.M., Gottfried, M.D., Hieronymus, T.L., Jinnah, Z. a, Ridgely, R., Ngasala, S.E., Temba, J., 2010. The evolution of mammal-like crocodyliforms in the Cretaceous Period of Gondwana. Nature 466, 748–751. doi:10.1038/nature09061
- O'Connor, P. M., J. W. Sertich, and F. K. Manthi. 2011. A pterodactyloid pterosaur from the Upper Cretaceous Lapurr Sandstone. Annals of the Brazillian Academy of Sciences 83:309–315.
- Odah, H., 2004. Paleomagnetism of the Upper Cretaceous Bahariya Formation, Bahariya Oasis. J. Appl. Geophys. 3, 177–187.
- Ogg, J.G., Hinnov, L.A., 2012. Cretaceous, in: Gradstein, F.M., Ogg, J.G., Schmidtz, M.D., Ogg, G.M. (Eds.), The Geologic Timescale 2012, Vol. 2. pp. 793–853.
- Peirce, J.W., Lipkov, L., 1988. Structural interpretation of the Rukwa Rift, Tanzania. Geophysics 53, 824–836. doi:10.1190/1.1442517
- Roberts, E.M., O'Connor, P.M., Gottfried, M.D., Stevens, N., Kapalima, S., Ngasala, S., 2004. Revised stratigraphy and age of the Red Sandstone Group in the Rukwa Rift Basin, Tanzania. Cretac. Res. 25, 749–759. doi:10.1016/j.cretres.2004.06.007
- Roberts, E.M., O'Connor, P.M., Stevens, N.J., Gottfried, M.D., Jinnah, Z.A., Ngasala,

- S., Choh, A.M., Armstrong, R.A., 2010. Sedimentology and depositional environments of the Red Sandstone Group, Rukwa Rift Basin, southwestern Tanzania: New insight into Cretaceous and Paleogene terrestrial ecosystems and tectonics in sub-equatorial Africa. J. African Earth Sci. 57, 179–212. doi:10.1016/j.jafrearsci.2009.09.002
- Roberts, E.M., Stevens, N.J., O'connor, P.M., Dirks, P., Gottfried, M.D., Clyde, W.C., Armstrong, R.A., Kemp, A.I.S., Hemming, S., 2012. Initiation of the western branch of the East African Rift coeval with the eastern branch. Nat. Geosci. 5, 289–294.
- Ryan, W.B.F., Bolli, H.M., Foss, G.N., Natland, J.H., Hottman, W.E., Foresman, J.B., 1978. Objectives, principal results, operations and explanatory notes of Leg 40, South Atlantic. Initial reports Deep sea Drill. Proj. 40, 5–28.
- Sadler, P. 1981. Sediment Accumulation Rates and the Completeness of Stratigraphic Sections. Journal of Geology 89:569–584.
- Sallam, H. M., E. Gorscak, P. M. O'Connor, I. A. El-Dawoudi, S. El-Sayed, S. Saber, M. A. Kora, J. J. W. Sertich, E. R. Seiffert, M. C. Lamanna. New Egyptian sauropod reveals Late Cretaceous dinosaur dispersal between Europe and Africa. Nature Ecology and Evolution. Accepted.
- Sampson, S.D., Witmer, L.M., Forster, C.A., Krause, D.W., Connor, P.M.O., Dodson, P., 1998. Predatory dinosaur remains from Madagascar: Implications for the Cretaceous biogeography of Gondwana. Science 80. 280, 1048–1051. doi:10.1126/science.280.5366.1048
- Saradeth, S., Soffel, H., Schult, A., 1987. Paleomagnetism of sedimentary rocks of the

- uppermost Cretaceous from the oases of Dakhla and Kharga in the Western Desert of Egypt. J. Geophys. 61, 64–66.
- Schult, A., Soffel, H.C., Hussain, A.G., 1978. Paleomagnetism of Cretaceous Nubian sandstone, Egypt. J. Geophys. 44, 333–340.
- Schult, A., Hussain, A.G., Soffel, H.C., 1981. Paleomagnetism of upper Cretaceous volcanics and Nubian sandstones of Wadi-Natash, SE Egypt and implications for the polar wander path for Africa in the Mesozoic. J. Geophys. 50, 16–22.
- Scotese, C.R., 2001. Atlas of Earth History, PALEOMAP project. Arlington, TX.
- Sereno, P.C., Wilson, J.A., Conrad, J.L., 2004. New dinosaurs link southern landmasses in the Mid-Cretaceous. Proceedings.Biological Sci. / R. Soc. 271, 1325–1330. doi:10.1098/rspb.2004.2692
- Sertich, J.J.-W., O'Connor, P.M., 2014. A new crocodyliform from the middle

 Cretaceous Galula Formation, southwestern Tanzania. 1. J. Vertebr. Paleontol. 34,

 576–596. doi:10.1080/02724634.2013.819808
- Snelling, N.J., 1965. Age determinations on three African carbonatites. Nature 205, 491.
- Spandler, C., Hammerli, J., Sha, P. Hilbert-Wolf, H.L., Hu, Y., Roberts, E.M., and Schmitz, M. MKED1: A new titanite standard for in situ microanalysis of trace elements, Sm-Nd isotopes, and U-Pb geochronology: Chemical Geology 425: 110-126.
- Stanhope, M.J., Waddell, V.G., Madsen, O., de Jong, W., Hedges, S.B., Cleven, G.C., Kao, D., Springer, M.S., 1998. Molecular evidence for multiple origins of Insectivora

- and for a new order of endemic African insectivore mammals. Proc. Natl. Acad. Sci. U. S. A. 95, 9967–9972. doi:10.1073/pnas.95.17.9967
- Stevens, N.J., O'Connor, P.M., Gottfried, M.D., Roberts, E.M., Ngasala, S., Dawson, M.R., 2006. Metaphiomys (Rodentia: Phiomyidae) From the Paleogene of Southwestern Tanzania. J. Paleontol. 80, 407–410. doi:10.1666/0022-3360(2006)080[0407:MRPFTP]2.0.CO;2
- Stevens, N.J., Gottfried, M.D., Roberts, E.M., Kapilima, S., Ngasala, S., O'Connor, P.M., 2008. Paleontological Exploration in Africa, in: Elwyn Simons: A Search for Origins. Springer, pp. 159–180.
- Stevens, N., Holroyd, P., Roberts, E., O'Connor, P., Gottfried, M., 2009 (a). *Kahawamys mbeyaensis* (n. gen., n. sp.) (Rodentia: Thryonomyoidea) from the Late Oligocene Rukwa Rift Basin, Tanzania. J. Vertebr. Paleontol. 29, 631–634. doi:10.1671/039.029.0219
- Stevens, N.J., O'Connor, P.M., Roberts, E.M., Gottfried, M.D., 2009 (b). A hyracoid from the late Oligocene Red Sandstone Group of Tanzania, Rukwalorax jinokitana (gen. et sp. nov.). J. Vertebr. Paleontol. 29, 972–975. doi:10.1671/039.029.0302
- Stevens, N.J., Seiffert, E.R., O'Connor, P.M., Roberts, E.M., Schmitz, M.D., Krause, C., Gorscak, E., Ngasala, S., Hieronymus, T.L., Temu, J., 2013. Palaeontological evidence for an Oligocene divergence between Old World monkeys and apes.

 Nature 497, 611–4. doi:10.1038/nature12161
- Stockley, G.M., 1932. The Geology of the Ruhuhu Coalfields, Tanganyika Territory. Q. J. Geol. Soc. 88, 610–NP. doi:10.1144/GSL.JGS.1932.088.01-04.20

- Strganac, C., Salminen, J., Jacobs, L.L., Polcyn, M.J., Ferguson, K.M., Mateus, O., Schulp, A.S., Morais, M.L., Tavares, T. da S., Gonçalves, A.O., 2014. Carbon isotope stratigraphy, magnetostratigraphy, and ⁴⁰Ar/³⁹Ar age of the cretaceous South Atlantic coast, Namibe Basin, Angola. J. African Earth Sci. 99, 452–462. doi:10.1016/j.jafrearsci.2014.03.003
- Swinton, W.E., 1950. Fossil eggs from Tanganyika, Illustrated London News.
- Taquet, P., 1976. Ostéologie d'Ouranosaurus nigeriensis, Iguanodontide du Crétacé Inférieur du Niger. Géologie Paléontologie du Gisem. Gadoufaoua (Aptien du Niger), Chapitre 3, 57–168.
- Tarduno, J.A., 1990. Brief reversed polarity interval during the Cretaceous Normal Polarity Superchron. Geology 18, 683–686. doi:10.1130/0091-7613(1990)018<0683:BRPIDT>2.3.CO;2
- Tarduno, J. a., W. Lowrie, W. V. Sliter, T. J. Bralower, and F. Heller. 1992. Reversed polarity characteristic magnetizations in the Albian Contessa Section, Umbrian Apennines, Italy: Implications for the existence of a Mid-Cretaceous mixed polarity interval. Journal of Geophysical Research 97:241–271.
- Tauxe, L., 2011. PmagPy, software package.
- Tauxe, L., Kent, D.V., 2004. A simplified statistical model for the geomagnetic field and the detection of shallow bias in paleomagnetic inclinations: was the ancient magnetic field dipolar? Timescales of the Paleomagnetic Field, 101-115. doi: 10.1029/145GM08

- Tauxe, L., Watson, G.S., 1994. The foldtest: an eigen analysis approach. Earth Planet. Sci. Lett. 122, 331–341.
- Tauxe, L., Banerjee, S.K., Butler, R.F., van der Voo, R., 2016. Essentials of Paleomagnetism, 4th web ed. ed.
- Torsvik, T.H., Van der Voo, R., Preeden, U., Mac Niocaill, C., Steinberger, B.,

 Doubrovine, P.V., van Hinsbergen, D.J.J., Domeier, M., Gaina, C., Tohver, E.,

 Meert, J.G., McCausland, P.J.A., Cocks, L.R.M., 2012. Phanerozoic polar wander,
 palaeogeography and dynamics. Earth-Science Reviews, 114, 325-368.
- Van der Beek, P., Mbede, E., Andriessen, P., Delvaux, D., 1998. Denudation history of the Malawi and Rukwa Rift flanks (East African Rift System) from apatite fission track thermochronology. J. African Earth Sci. 26, 363–385.
- Wack, M., 2010. A new software for the measurement of magnetic moments using SQUID and spinner magnetometers. Comput. Geosci. 36, 1178–1184. doi:10.1016/j.cageo.2010.05.002
- Wang, T., Ramezani, J., Wang, C., Wu, H., He, H., Bowring, S.A., 2016. High-precision U–Pb geochronologic constraints on the Late Cretaceous terrestrial cyclostratigraphy and geomagnetic polarity from the Songliao Basin, Northeast China. Earth Planet. Sci. Lett. 446, 37–44. doi:10.1016/j.epsl.2016.04.007
- Watson, G.S., 1956. A test for randomness of directions. Geophys. Suppl. to Mon. Not. R. Astron. Soc. 7, 160–161.
- Wescott, W.A., Krebs, W.N., Engelhardt, D.W., Cunningham, S.M., 1991. New

Biostratigraphic Age Dates from the Lake Rukwa Rift Basin in Western Tanzania: Geologic Note. Am. Assoc. Pet. Geol. Bull. 75, 1255–1263.

Wilson, J.A., Sereno, P.C., Srivastava, S., Bhatt, D.K., Khosla, A., Sahni, A., 2003. A new abelisaurid (Dinosauria, Theropoda) from the Lameta Formation (Cretaceous, Maastrichtian) of India. Contrib. From Museum Paleontol. Univ. Michigan 31, 1–42.

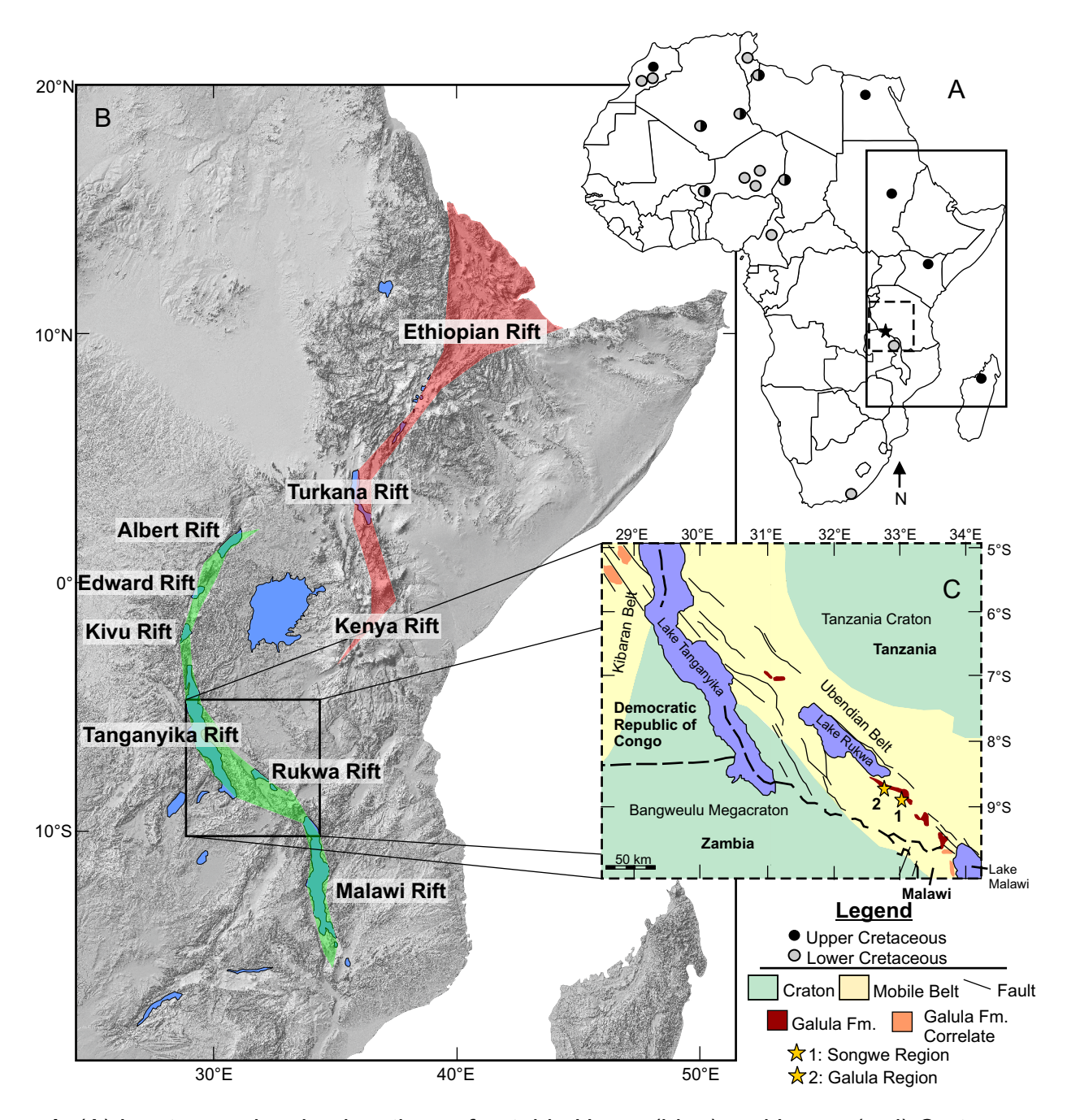


Figure 1: (A) Inset map showing locations of notable Upper (blue) and Lower (red) Cretaceous terrestrial vertebrate fossil localities in Africa, with the Galula Formation shown in black (Based on Stevens et al., 2008) and regions shown in (B) and (C). (B) Location of the East African Rift System, showing individual rift segments comprising the Eastern (red) and Western (green) branches. (C) Simplified structural and basement geology map of the Rukwa Rift segment. General locations of Archaean cratons (light green) and Proterozoic mobile belts (light yellow) are shown along with major faults. Known exposures of the Galula Formation are shown in red and potentially correlative sequences in the DRC and Malawi are shown in pink. Regions where paleomagnetic samples were collected for this study are indicated by yellow stars (sedimentary exposures based on Roberts et al., 2010, fig. 1; basement geology based on Roberts et al. 2012, fig. 1).

Table 1: Galula Formation vertebrate fauna. Based on O'Connor et al. (2006) and Roberts et al. (2010), unless otherwise indicated.

Namba Member		Mtuka Member	
Taxon	Reference	Taxon	Reference
Osteichthyes		Osteichthyes	-
Actinopterygii		Sarcopterygii	-
Teleostei		Dipnoiformes	-
Osteoglossomorpha		Dipnoi	_
Teleostei indet.		Ceratodontidae	-
Sauropsida		Lupaceradotus useviaensis	Gottfried et al. (2009
Testudines		Sauropsida	-
Crocodyliformes		Testudines	_
Notosuchia		Crocodyliformes	-
Pakasuchus kapilimai	O'Connor et al. (2010)	Dinosauria (non-avian)	-
Notosuchia indet.		Saurischia	_
Peirosauridae		Theropoda indet.	-
Rukwasuchus yajabalijekendu	Sertich and O'Connor (2014)		-
Dinosauria (non-avian)		Sauropoda	-
Saurischia		Titanosauria	-
Theropoda indet.		Dinosaur eggshell?	-
Sauropoda			
Titanosauria			
Rukwatitan bisepultus	Gorscak et al. (2014)		
Dinosaur eggshell			
Oofamily Megaloothidae	Gottfried et al. (2004)		
Mammalia	<u></u>		
Gondwanatheria			
Sudamericidae	Krause et al. (2003)		

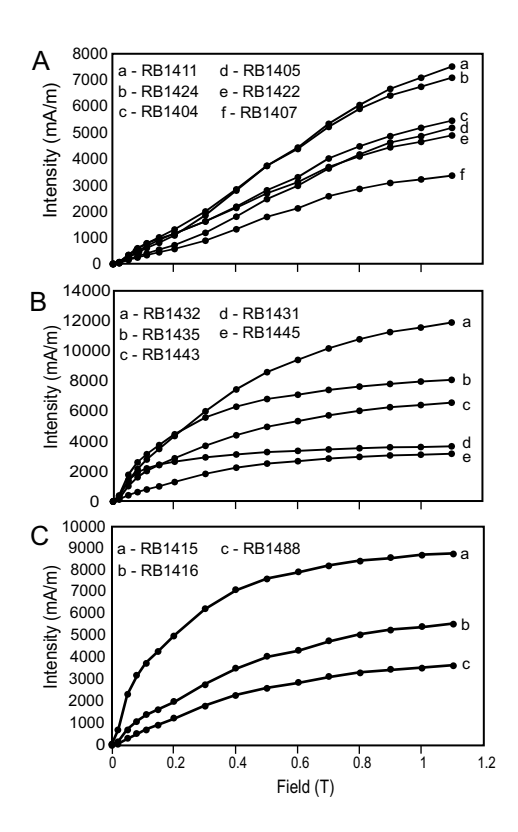


Fig. 2: IRM acquisition curves for (A) TZ-07 (Namba Member), (B) Mtuka Member, (C) Other Namba Member sites: Hamposia River (RB14415 and RB1416) and Galula Fm. – Nsungwe Fm. contact site (RB1488).

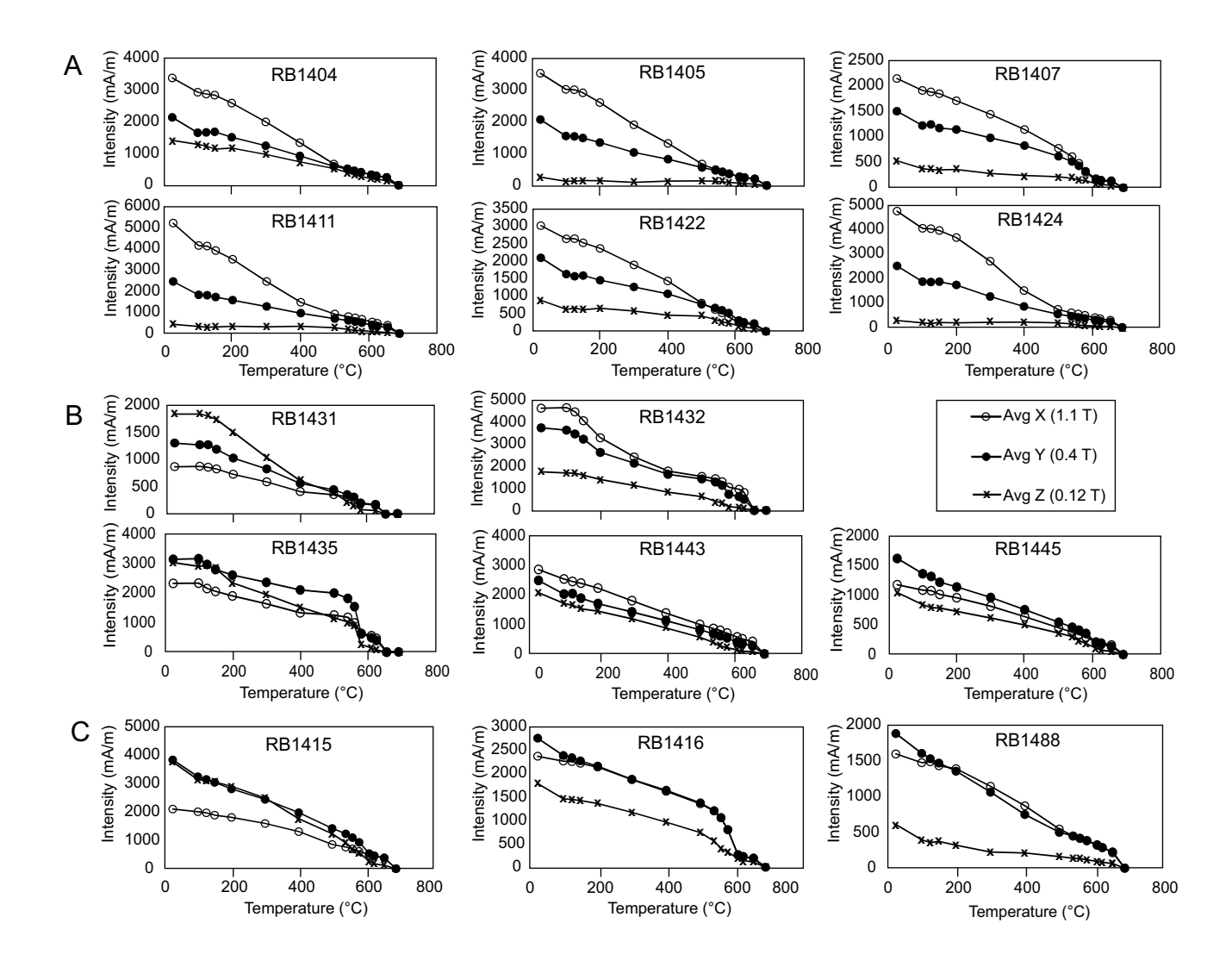


Fig. 3: IRM demagnetization curves for (A) TZ-07 (Namba Member), (B) Mtuka Member, (C) Other Namba Member sites: Hamposia River (RB14415 and RB1416) and Galula Fm. – Nsungwe Fm. contact site (RB1488).

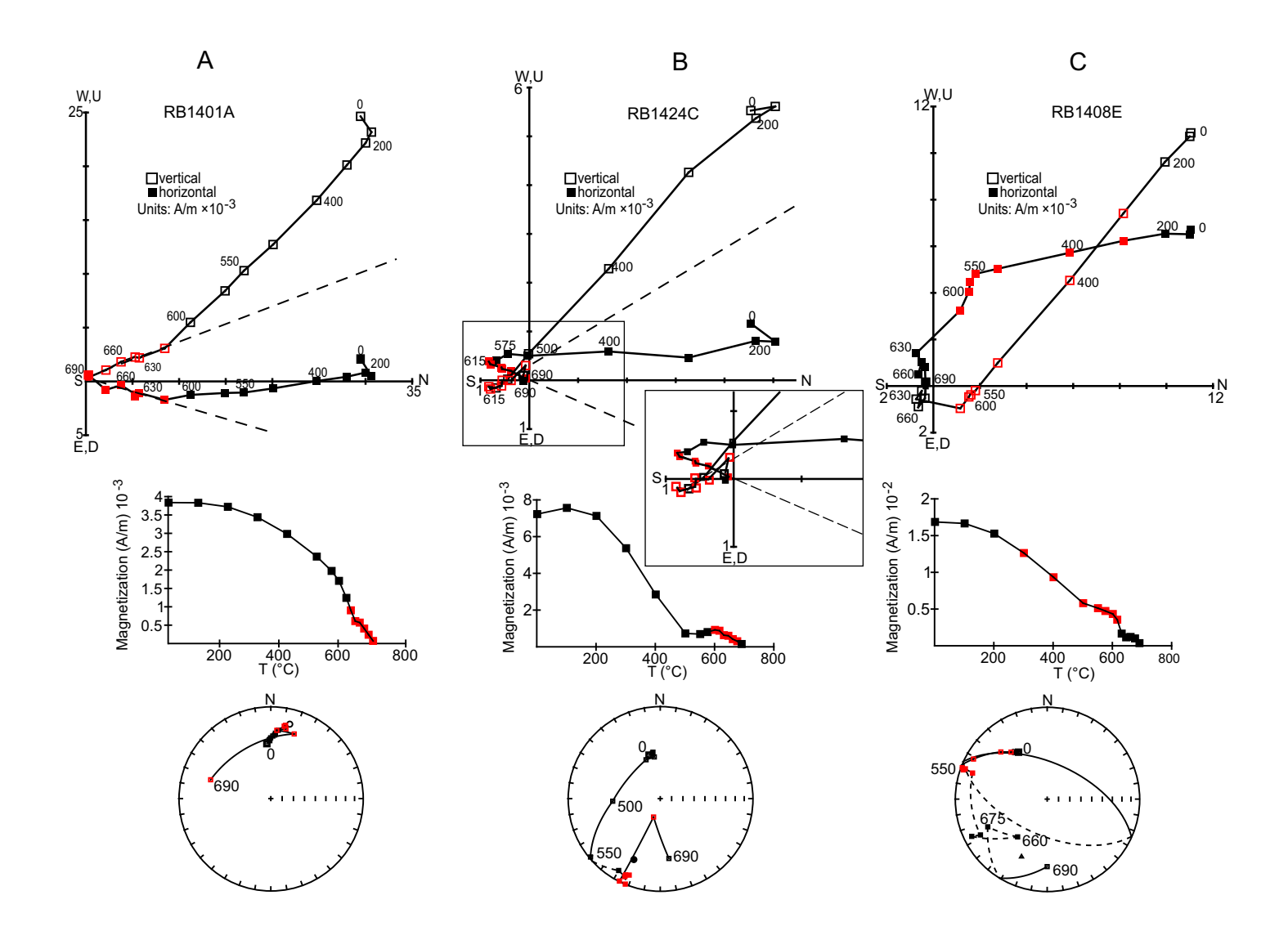


Fig. 4: Vector end point diagrams (top), intensity plots (middle) and equal area projections showing thermal demagnetization of select Namba Member samples. (A) Normal polarity, characterized using PCA. (B) Reversed polarity, characterized using PCA, inset highlighting high temperature steps. (C) Reversed polarity, characterized using GC. Top row: closed (open) symbols indicate declination (inclination), dotted line is a best fit through selected points. Bottom row: closed (open) symbols indicate positive (negative) inclination. Red points are selected steps.

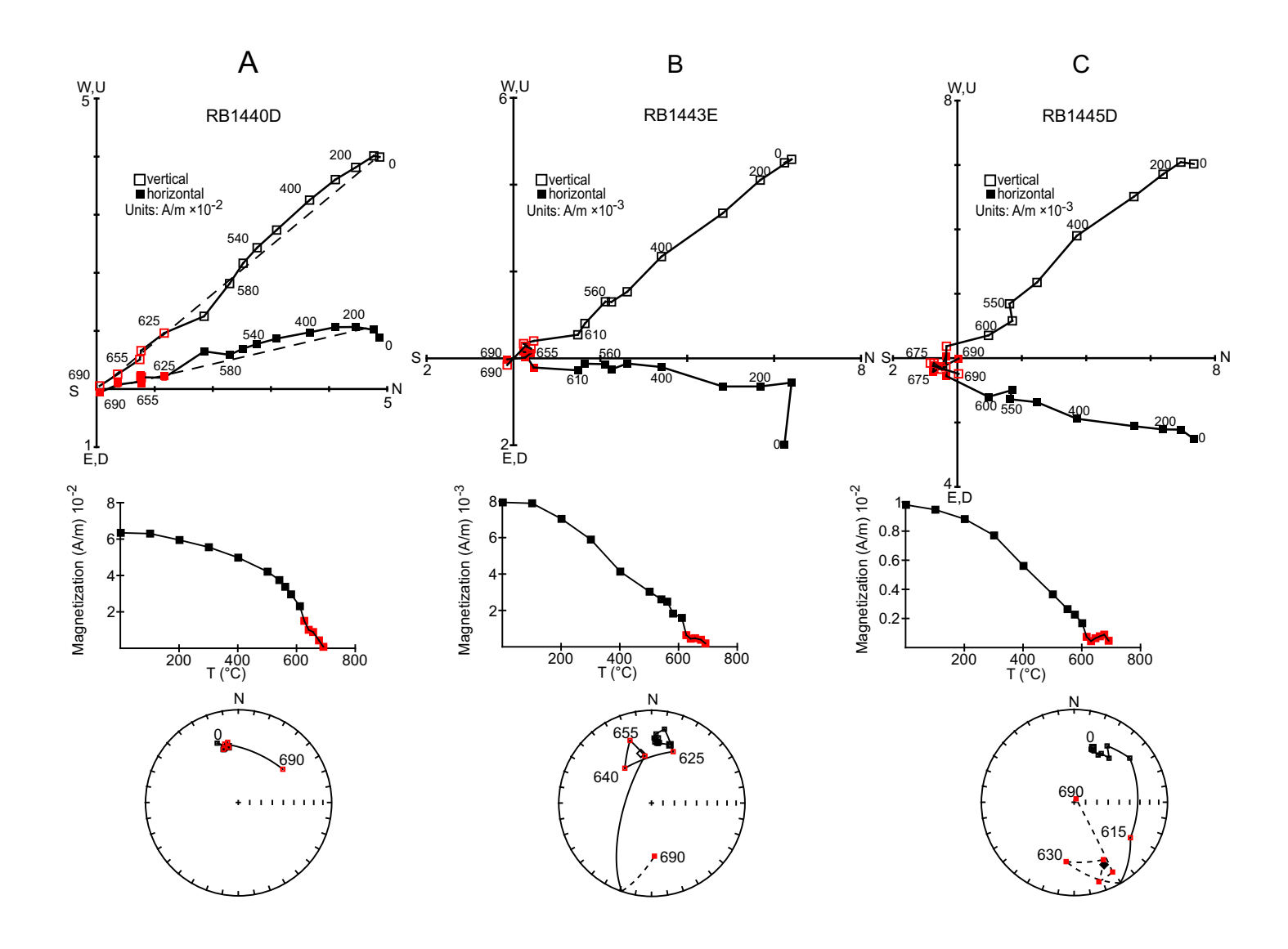


Fig. 5: Vector end point diagrams (top), intensity plots (middle) and equal area projections (bottom) showing thermal demagnetization of select Mtuka Member samples. (A) Normal polarity, characterized using PCA. (B) Normal polarity, characterized using Fisher mean. (C) Reversed polarity belonging to a mixed polarity site, characterized using Fisher mean. Top row: closed (open) symbols indicate declination (inclination), dotted line is a best fit through selected points. Bottom row: closed (open) symbols indicate positive (negative) inclination. Red points are selected steps.

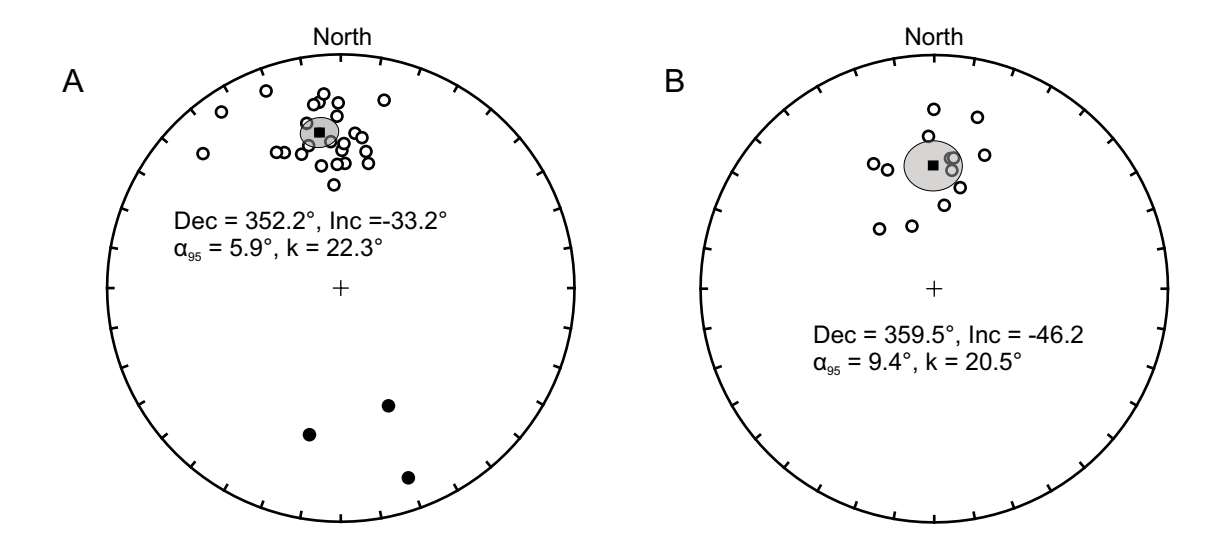


Fig. 6: Paleomagnetic site directions from the Namba (A) and Mtuka (B) members. Closed (open) circles indicate positive (negative) inclination. Squares and shaded circles indicate mean directions and α_{95} confidence ellipses for all alpha and beta level sites, with reversed sites inverted. All directions are shown in tilt-corrected coordinates.

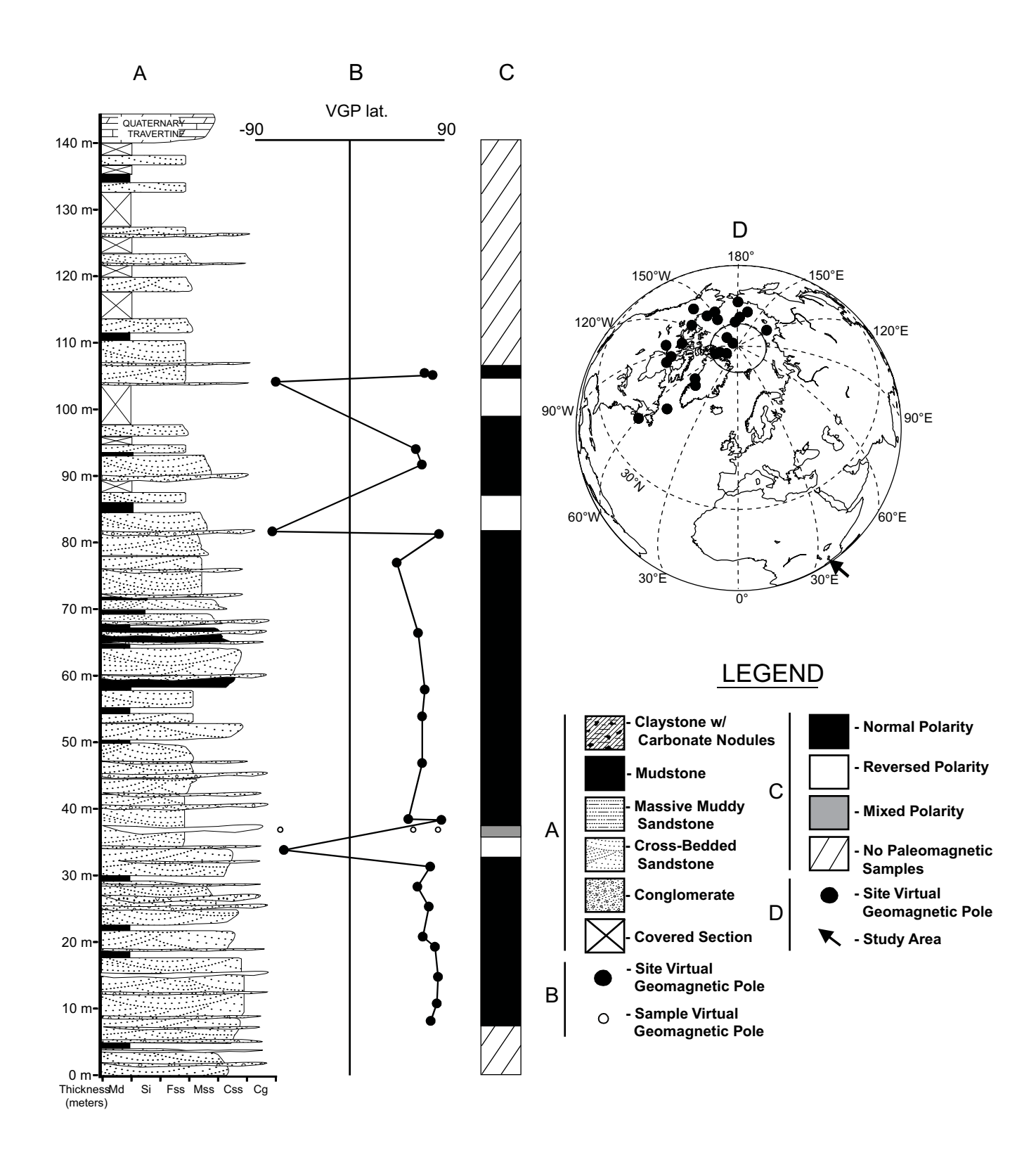


Fig. 7: (A) TZ-07 stratigraphic section (Roberts et al. 2004; Fig. 5) plotted next to (B) virtual geomagnetic pole (VGP) latitude, (C) inferred polarity, and (D) VGP positions (reversed sites inverted).

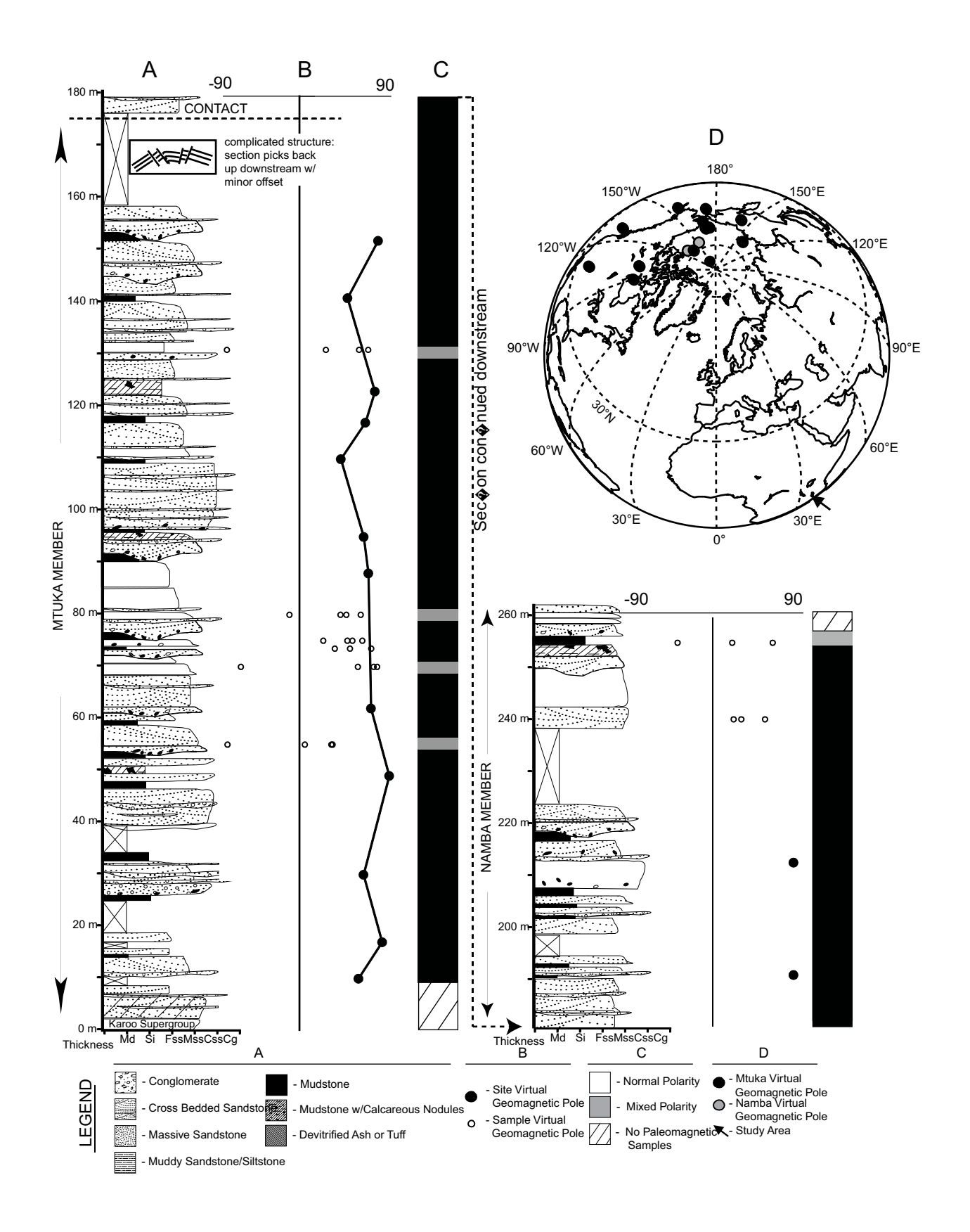


Fig. 8: (A) Mtuka River stratigraphic section (Roberts et al., 2010; Fig. 7) plotted next to (B) virtual geomagnetic pole (VGP) latitude, (C) inferred polarity, and (D) VGP positions.

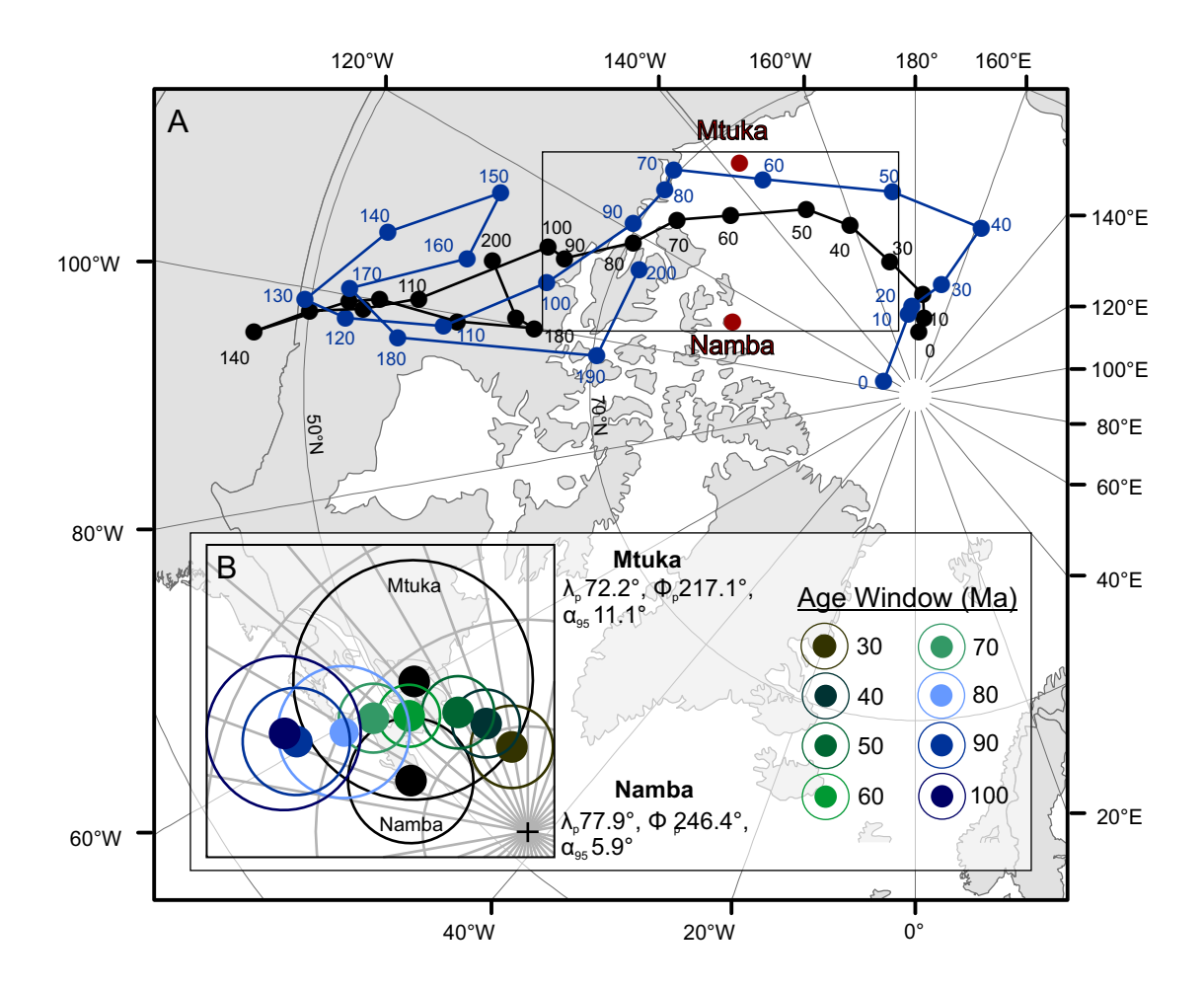


Fig. 9: (A) 200 Myr master apparent polar wander path (APWP) for Africa (Besse and Courtillot, 2003; black) and 200 Myr APWP for Gondwana in South African coordinates (Torsvik et al., 2012; blue) with paleomagnetic poles calculated for the Mtuka and Namba members (red). (B) Rectangle outlines poles from Besse and Courtillot (2003) that overlap with either member with α95 confidence ellipses.

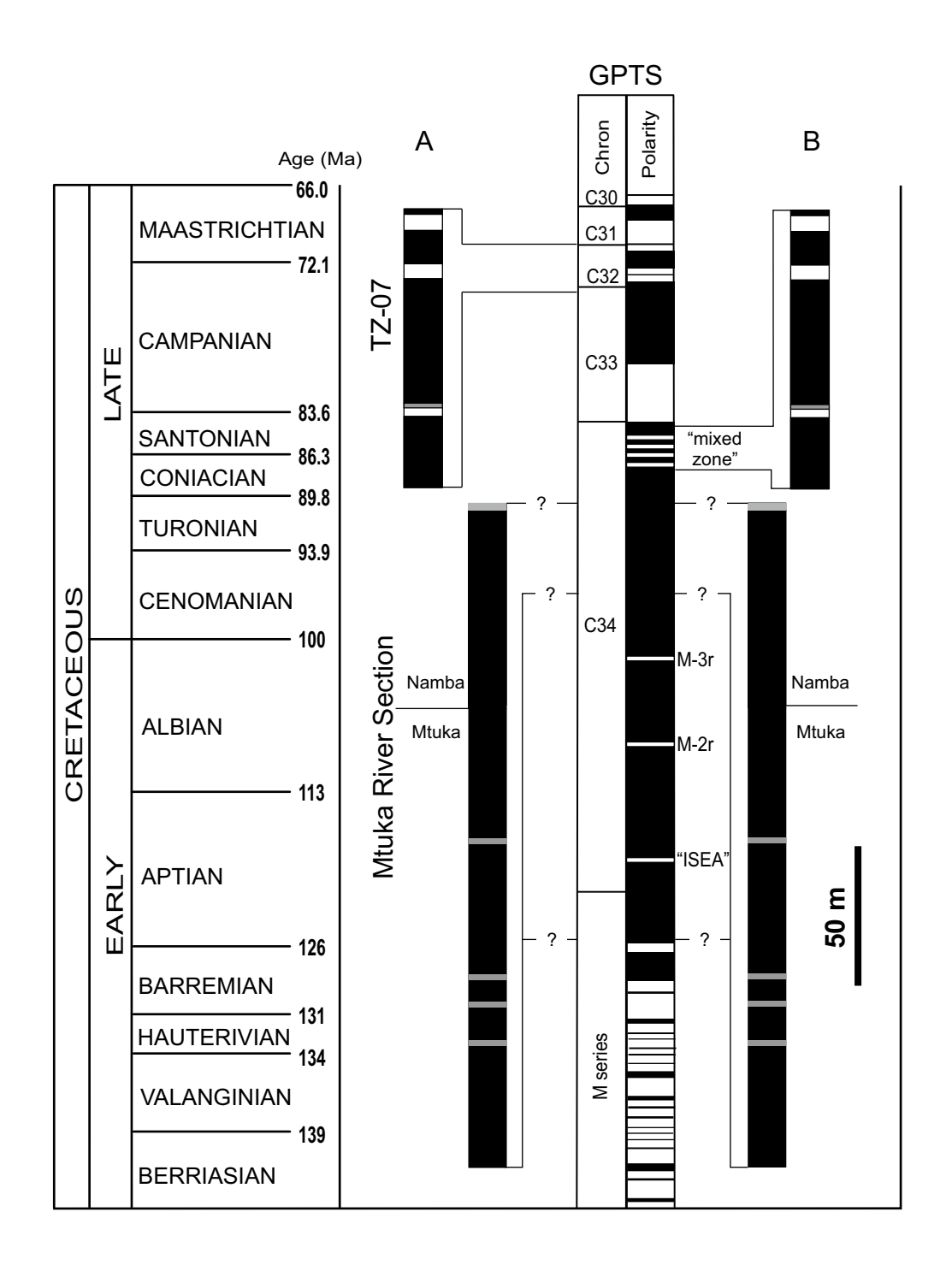


Fig. 10: Stratigraphic correlations to the GPTS. (A) Namba Member reversals correlated to C32 in the Campanian (preferred correlation) (B) Namba Member reversals correlated to short excursions during the end of the CNS (Guzhikov et al., 2003; Montgomery et al., 1998; Wang et al., 2016). The timing of these reversals is poorly constrained and represented here as a "mixed polarity" zone. Ages are based on Ogg and Hinnov (2012).

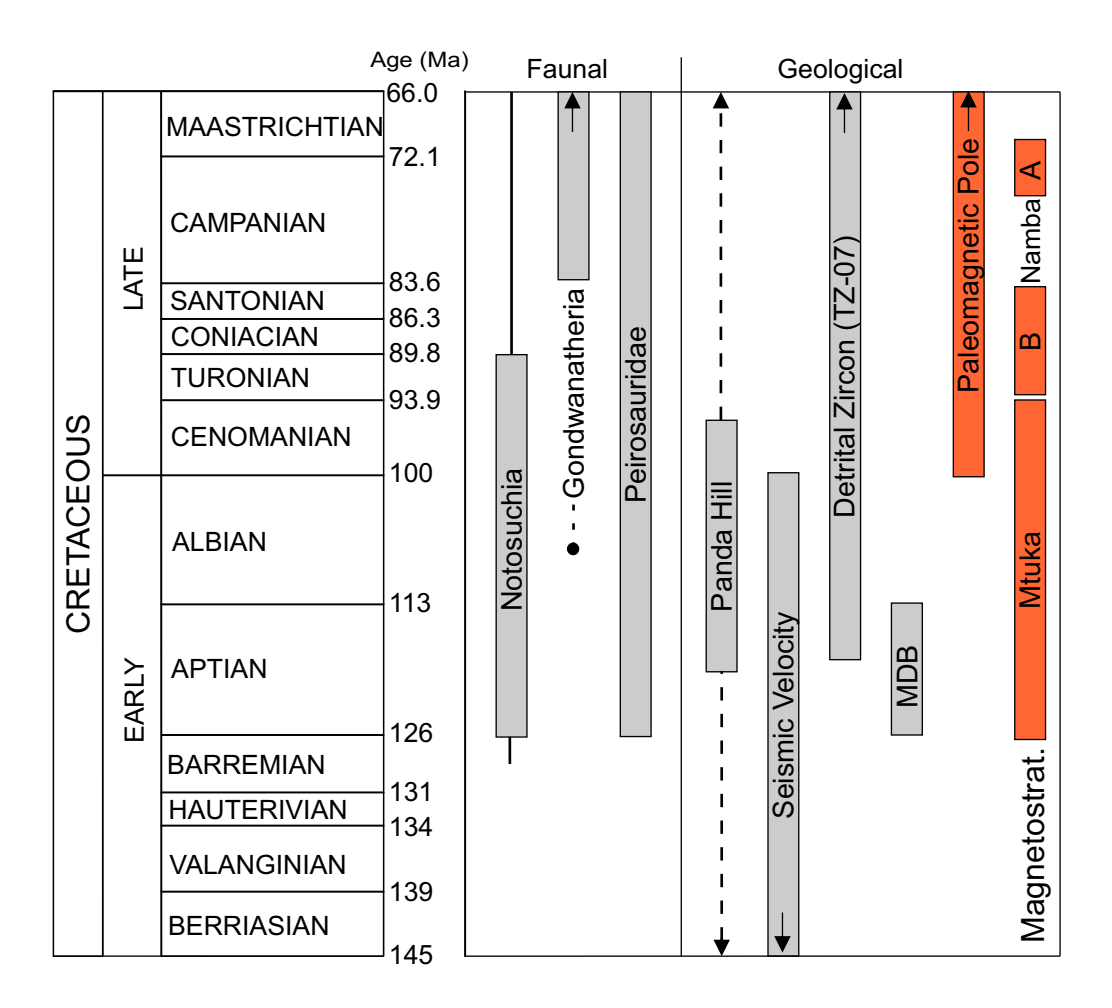


Fig. 11: Age constraint for the Galula Formation. Temporal ranges of taxa with first or last appearances in the Cretaceous. All taxa shown are from the Namba Member. For Notosuchia, grey bar indicates the range for the "Mariliasuchus- Adamantinasuchus- Malawisuchus-Candidodon" clade of O'Connor et al. (2010). Black line indicates known range for all Notosuchia. For Gondwanatheria, grey bar indicates range for the group and the point indicates the estimated divergence time for Sudamericidae and other gondwanatherians (from Krause et al. (2014)). Dashed lines surrounding the Panda Hill reflect uncertainty concerning initiation and reactiviation of carbonatite volcanism in the region. Arrows indicate ranges that extend beyond the Cretaceous. MDB = Malawi Dinosaur beds. Ranges in red are from this study. "Namba A" and "Namba B" refer to alternate correlations for the upper Namba Member (see text).